https://doi.org/10.5194/egusphere-2026-4137
Preprint. Discussion started: 1 September 2026

Improvements of a subcanopy snow model and its interception conveyed by observations from a mid-altitude alpine site

Thomas Pauze[1], Axel Bouchet[1], Isabelle Gouttevin[1], Aaron Boone[2], Mathieu Fructus[1], Matthieu Lafaysse[1], Erwan Le Gac[1], Agnès Rivière[3], and Yves Lejeune[1]

[1]Météo-France, CNRS, Univ. Grenoble Alpes, Univ. Toulouse, CNRM, Centre d'Études de la Neige, 38000 Grenoble, France
[2]Météo-France, CNRS, Univ. Grenoble Alpes, Univ. Toulouse, CNRM, Toulouse, France
[3]Mines Paris, PSL University, Centre for Geosciences and Geoengineering, Fontainebleau, France

Correspondence: Thomas Pauze (thomas.pauze@meteo.fr)

Abstract. Understanding the accumulation and melt of snow is essential to capture the hydrology of mountainous areas. Forests impact significantly the amount of snow on the ground through diverse processes, including the interception of snowfall. The Multi-Energy-Balance (MEB) module within the SURFEX/ISBA surface model has been designed to capture these impacts for climate applications. However, the original version of MEB coupled with the physically-based snow model Crocus (MEB/Crocus) fails to reproduce the subcanopy snow dynamics observed at Col de Porte, a mid-altitude alpine snow observatory. In this study, based on new observations at Col de Porte and recent literature, we propose an enhanced version of MEB/Crocus by revisiting solid interception processes : maximum interception, interception rate, unloading and melt. This new version reduces the positive bias of subcanopy simulations by at least 40% for snow water equivalent and snow depth, through an enhanced interception, longer interception duration and associated sublimation and melt. The wide range of observations at Col de Porte furthermore confirms that MEB/Crocus has a satisfactory representation of the different processes involving the forest cover, including vegetation temperatures, ground temperatures and radiation under forest. With this new version of MEB/Crocus, the model's net performance remains unchanged -or is even slightly improved- at boreal sites. We also take the opportunity to use new observations to explore the sensitivity of the model to a top-of-canopy forcing in wind and air temperature. While forcing the model with air temperature from above the canopy is found to have no significant impact, having a top-of-canopy wind is key to the representation of the evolution of snow under forest as it strongly affects the sensible and latent heat fluxes. The improvements and enhanced understanding of the model sensitivity pave the ground to extending the applications of MEB, from climate to the hydrology of mid-latitude mountainous areas.

1 Introduction

Snow is a key driver of the hydrological cycle in mountainous areas. It affects the total streamflow and the timing of the maximum of the seasonal runoff. In north-western America, 50–80% of runoff occurs during the snowmelt period (Stewart et al., 2004), and most of the northern hemisphere depends on snowmelt-derived streamflow (Stewart, 2009; Armstrong et al., 2019; Li et al., 2017; Barnett et al., 2005). Understanding the timing and amount of snowmelt is hence critical to predict streamflow peaks and floods and manage freshwater resources. Furthermore, about 23% of the land surface is subject to snowfall over

https://doi.org/10.5194/egusphere-2026-4137
Preprint. Discussion started: 1 September 2026

forested areas (Deschamps-Berger et al., 2025). The presence of trees affects the mass balance and energy budget of snowpacks: trees absorb shortwave radiation, reducing the amount of such radiation received by the underlying snowpack while increasing the downwelling longwave radiation at the surface (Gouttevin et al., 2015). Moreover, snowfall is intercepted by the canopy (Helbig et al., 2020; Hedstrom and Pomeroy, 1998) and may sublimate (Pomeroy et al., 1998) or melt (Mahat and Tarboton, 2014) before unloading, thus reducing the amount of snow reaching the ground. The resulting shallower subcanopy snowpack depth is then generally lower than adjacent non-forested areas, and it has different microstructural properties (Bouchard et al., 2022). As a consequence of these processes, the evolution of snow under forests differs from that in open areas (Lundquist et al., 2021; Molotch et al., 2016; Mazzotti et al., 2019), also leading to discrepancies in the hydrological behaviour of catchments dominated by snow under forest (Molotch et al., 2009). Henceforth, models developed to ensure an accurate representation of runoff in forested catchments with seasonal snow cover need to accurately capture snow-canopy interactions.

Snow also plays an important role in the global climate system. One of its main impacts is on the surface radiative budget (Flanner et al., 2011) - an effect that is considerably altered by the presence of forests. It is therefore crucial to take the canopy effects into account to understand and model the snow albedo feedback, which explains much of the variation in the projected warming of Northern Hemisphere land surface areas (Abe et al., 2017; Thackeray et al., 2014).

Due to the significant impact of forest on snow and climate modelling, and following the SNOWMIP2 intercomparison project (Essery et al., 2009; Rutter et al., 2009), a new parameterization has been developed for nature-tiles within the model representing the interactions between the soil-biosphere-atmosphere (ISBA): ISBA-MEB (Boone et al., 2017). It couples a multi-layer and physical based snowpack model overlying a variable-layer soil scheme, with an explicit litter layer, a bulk vegetation scheme, and the atmosphere. As such, ISBA-MEB hence represents all the processes inherent to canopy-snow interactions, including the intercepted mass of water, whether solid or liquid; how they evolve in the canopy and unload from the canopy, as well as the impact of canopies on radiative and turbulent fluxes. The vegetation module MEB models these processes, coupled with a snow model available within ISBA such as the intermediate-complexity Explicit Snow model (Decharme et al., 2016) for large-scale, climate-oriented applications, or the detailed, physics-based Crocus snow scheme (Lafaysse et al., 2025). This last coupled model is referred to as MEB/Crocus henceforth in this article.

MEB has been developed and tested in boreal forest environments. Napoly et al. (2020) used the BERMS dataset from the Canadian boreal forest (Bartlett et al., 2006; Krinner et al., 2018; Ménard et al., 2019) to validate the explicit representation of canopy processes in MEB, which were previously miscaptured by ISBA using a composite bulk snow scheme, as well as by several classic land-surface models taking part in the SnowMIP2 intercomparison project to validate explicit processes (Essery et al., 2009; Rutter et al., 2009). The MEB developments improved the snow depth simulations, especially during the melt period, with a better representation of the melt-out date. Nousu et al. (2024) used data from two Finnish sites to validate the surface energy budget and snowpack simulation at forest sites with MEB/Crocus. These articles demonstrate the general validity of the MEB scheme and MEB/Crocus coupling for the boreal regions. However, the behaviour of the MEB/Crocus coupled model has not been thoroughly evaluated in alpine regions, where forest structure and climate differ from boreal conditions. A preliminary study by Vincent et al. (2018) showed that MEB/CROCUS exhibits significant snow depth biases at an alpine site which could not be attributed to uncertainties in vegetation parameters or forest vegetation density spatial variability. The two potential causes for this bias highlighted in this study were an inadequate scheme for snow interception and the representation of melt or unloading of the intercepted snow. Recent intercomparisons between MEB-Crocus and benchmark FSM2ohsd simulations over a 1200 km^2 domain in Swiss Alps suggest that the limitations identified at this site may be representative at larger scale in dense Alpine forests (Mazzotti et al., 2026).

Recent observations in alpine climates have guided the development of more accurate representations of snow under forests. Especially, progress has been made in representing radiation under the canopy, with important fieldwork campaigns conducted in Switzerland and Finland (Mazzotti et al., 2020a, b; Webster et al., 2016a), which used airborne LiDAR to precisely characterise subcanopy snow distributions. New metrics have also been developed to characterize forest properties. Incorporating these new metrics into revised parameterizations enabled a better simulation of distributed longwave (LW) and shortwave (SW) radiation under forest. On the other hand, despite recent studies (Cebulski and Pomeroy, 2025, 2026) that showed the sensitivity of interception to snow-leaf contact area and linked the unloading with canopy snow load, snowmelt and wind shear stress, the interception and unloading processes that have been identified as key to understanding the evolution of snow under forest (Lundquist et al., 2021), have so far only relied on limited observational data. Measurements taken over two winters (2016–2017 and 2017–2018) at the mid-altitude Col de Porte site in France as part of the SNow Under Forest (SNOUF) project (Sicart et al., 2023) -and continued from 2018 to the present- could contribute to a significant advance in understanding the processes governing snow interception and unloading. These measurements include spatially distributed data on radiation beneath the forest canopy, snow depth, snow water equivalent (SWE), and non-interception. A second source of uncertainty concerns the forcing data used to drive these models. While ISBA-MEB is designed to be forced by atmospheric conditions above the canopy, offline applications commonly rely instead on either atmospheric model data (e.g. reanalyses) or in-situ observations from nearby open areas at screen level, and the sensitivity of subcanopy simulations to the height and characteristics of the forcing data has been poorly addressed (Clark et al., 2015).

In this article, based on observations at Col de Porte, we explore how the ISBA-MEB model, developed primarily for large-scale hydrological, meteorological and climate applications in boreal forests, can be adapted to model sub-canopy snow in alpine forest and climate conditions. We make use of the version coupled to the detailed Crocus snow model. As a secondary objective, we also assess the impact of forcing the model with data from above the canopy, instead of nearby open-area screen-level observations. In a Data and Methods section, we first present the Col de Porte mid-altitude research site and the associated forest-stand observations, which were used for both global and detailed, process-based evaluation of the model. Ancillary boreal forest sites are also introduced, which enable further model evaluations. We then describe the ISBA-MEB/Crocus model, and the parameterization changes developed in the current study to adapt the model to better represent mid-altitude, Alpine conditions. In the result sections, we first examine the model sensitivity to forcing data representing top-of-canopy conditions. We then detail the improvements conveyed by the parameterizations adaptations and carry out a general model evaluation at the Col de Porte site, while verifying that the performances of the new model at boreal sites are minimally affected in terms of performance. Finally, we discuss the limitations of our approach and possible ways to further improve the understanding and modelling of canopy and snow interactions in alpine settings.

https://doi.org/10.5194/egusphere-2026-4137
Preprint. Discussion started: 1 September 2026

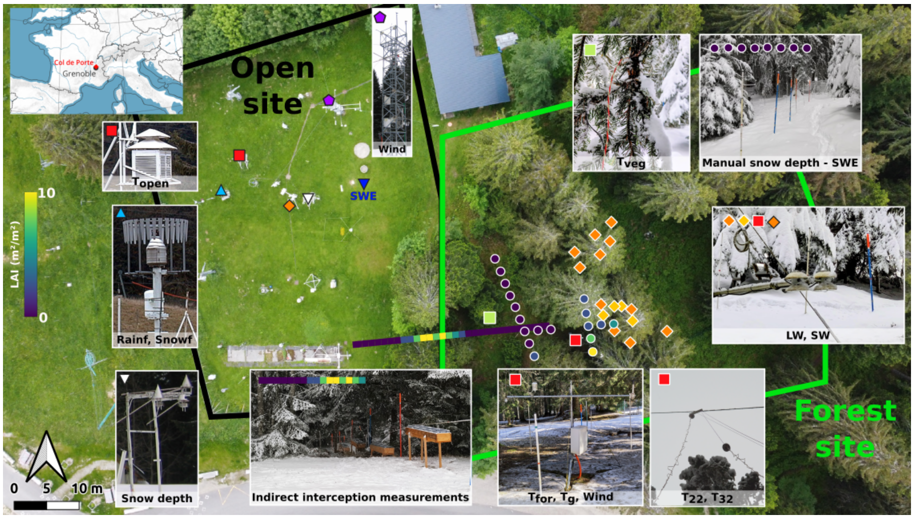

Figure 1. Aerial view of the Col de Porte observatory (1325m). In the open site (left) instruments are permanent and provide data at an hourly timestep since 1993. In the forest site (right), the manual observation of snow depth and SWE along transects (rounds with colors depending on LAI), the automatic weather station (red square) with wind, air temperature at 2m (Tfor), upward and downward LW and SW measurements and the ground temperature profile (Tg) have been installed since December 2016. In December 2022, the T22 and T32 air temperature and the vegetation temperature Tveg measurements were installed just above the automatic station. The orange diamonds (resp. yellow) represent the downward SW and LW radiometers (resp. the downward SW radiometers only) from the radiometer array installed during the winters 2016-2017 and 2017-2018. The indirect interception measurements transect was set up during the 2019-2020 winter (line with colors varying according to LAI). Global map background from OpenStreetMap.

2 Data and methods

2.1 In situ observations

2.1.1 Col de Porte : open site

The Col de Porte (CdP) site is a long-term, mid-altitude (1325 m, 45.30° N, 5.77° E) instrumented site located in the Chartreuse mountain range which is a part of the French Alps. For the 1994-2024 period, mean annual temperature is 6.9 °C and 1.2 °C during winter (from beginning of November to the end of March). The average annual precipitation is about 2000 $\mathrm{kg\,m^{-2}}$ with approximately one third falling as snow. There are two instrumented parcels (Fig. 1): an open field which has been taking measurements since 1959 described in Lejeune et al. (2019); and a forest stand with more recent instrumentation (dating back to 2016) detailed in Sicart et al. (2023) and Helbig et al. (2020).

The open site provides observations for all of the atmospheric near-surface variables needed to drive a snow model, namely: screen-level temperature (T_{open}) and relative humidity of air, 10 m wind speed, downward longwave (LW↓) and shortwave (SW↓) radiation fluxes, rainfall (Rainf) and snowfall (Snowf). For these latter two variables, as described in Lejeune et al.

https://doi.org/10.5194/egusphere-2026-4137
Preprint. Discussion started: 1 September 2026

(2019), the precipitation phase is computed from air temperature and expertly adjusted based on all relevant concomitant data (fresh snow depth measurements, snow depth variations, surface albedo, surface temperature, air temperature evolution and differences between heated and non-heated rain gauges). A correction for gauge undercatch is applied to the solid fraction of precipitation based on the WMO 1996 and 2018 recommendations (Forland et al., 1996; Nitu et al., 2019). All of these forcing variables are available at an hourly resolution since 1993. Validation data available for snow modeling in the open include hourly automatic snow depth, basal snowmelt measured with a lysimeter, soil temperatures at 5, 10, 20 and 30 cm depth, snow water equivalent (SWE, $\mathrm{kg\,m^{-2}}$) from a cosmic ray sensor (daily) and manual snow cores (weekly) as well as manual weekly snowpits. The open site measurements have been used in a number of snow related studies and especially for the development and evaluation of snow models, as in (Brun et al., 1989, 1992; Boone and Etchevers, 2001; Lafaysse et al., 2017), and including the SnowMIP and ESM-SnowMIP model intercomparison exercises (Etchevers et al., 2004; Ménard et al., 2019).

2.1.2 Col de Porte : forest site

The forest occupies about half of the total Col de Porte site area (Fig. 1) and is dominated by Norway spruce (Picea abies), with smaller and younger silver fir (Abies alba) present in the understory. Small deciduous trees are present near the east side of the main building; they do not affect the instrumentation. Like surrounding areas of the Chartreuse, the forest stand at CdP has been impacted by bark beetle infestation. Over the past five years, one tree has been felled due to infection, with no major impact on observations. The main trees within the study plot have an average height of approximately 35 m, with an average Leaf Area Index (LAI) of 4.5 $\mathrm{m^2\,m^{-2}}$ across the entire stand. We derived these estimations of forest characteristics from a LiDAR flight of the parcel and manual tree observations conducted during the SNOUF campaign, from data acquired at national scale over France within the LiDAR HD project (https://geoservices.ign.fr/lidarhd, last access 10/07/2026). Calculations were made using the lidR library (Roussel et al. (2020), see appendix A for more details). As the forest stand is mostly composed of coniferous species and varies very little over time, we assume a constant LAI over the past decade spanned by our simulations. LAI is an important parameter in the MEB/Crocus model used in this study, and the sensitivity of the modelled subcanopy snow depths to LAI is explored in Appendix A , showing that this sensitivity is consistent with the spread in subcanopy observations. Finally, a litter layer with a thickness of approximately 4 cm covers the forest soil. The forest area has been instrumented since December 2016 (Sicart et al., 2023). Meteorological variables are measured at an automatic weather station beneath the canopy (red square in the forest site in Fig. 1): air temperature at 2 m (T_{for}), humidity, radiation and wind. To describe the sub-canopy snowpack and energy balance, an automatic snow depth sensor, upward and downward SW and LW radiometers and two ground temperature (T_g) profiles (2.5 cm - in the litter, 8.5 cm, 15 cm, 30 cm, 60 cm) are installed at the weather station. To complete these classic observations and to characterize air temperature variations with height, two air temperature sensors were installed in December 2022 at 22 m (T_{22}) and 32 m(T_{32}) within the canopy, above the sub-canopy weather station. The highest of these observations, close to the canopy top, will be used to force the snow model and characterize the impact of above-canopy air temperature forcing onto the sub-canopy snowpack. To examine spatial variability of radiation under canopy, an array of radiometers measuring downward SW and LW was spread in the forest site over the two winters of the SNOUF campaign: 2016-2017 and 2017-2018 (orange and yellow diamonds in Fig. 1). In addition to meteorological observations, the

https://doi.org/10.5194/egusphere-2026-4137
Preprint. Discussion started: 1 September 2026

spatial distribution of SWE and snow depth has been characterized weekly since January 2017 through manual measurements along transects of 18 poles distributed below the forest (dots in forest site in Fig. 1). Manual SWE measurements stopped in April 2022 while snow depth measurements along the transects are still conducted every week. These data will be used to evaluate MEB/Crocus. We will also rely on a 1-year dataset of indirect interception measurements described in Sicart et al. (2023) and detailed hereafter (rectangles in forest site in Fig. 1). New boxes were installed during the 2019-2020 winter on a transect (East-West) starting in the open area and finishing well inside the forest parcel: the overlying canopy density varies considerably along this path. Shortly after a snowfall event, all the boxes were weighed and then emptied. By comparing SWE in open boxes and in sub-canopy ones, we deduce the snow intercepted by trees. Some measurements were also taken during the unloading phase, enabling to estimate directly the amount of unloaded snow. These measures are time-consuming and require significant human resources but give us remarkable insight into the dynamics of the solid interception reservoir. Measurements of vegetation temperature complement this sub-canopy instrumentation: 4 temperature sensors are installed on the trunk (T_{trunk}) and branches (T_{branch}) (south and north faces) of a medium-sized silver fir (Abies alba) with a height of $15\,\mathrm{m}$ located $5\,\mathrm{m}$south-west of the automatic weather station (see Fig. 1, green square). As the temperature sensors are not sheltered, they get heated by direct sunlight at the end of the morning, resulting in erroneous measurements. To avoid this issue, we removed 11am and 12am observations and replaced them with a second order polynomial (quadratic) interpolation. Moreover, the north and south sensors on branches and trunks behave similarly and show very close values; thus the vegetation temperatures were averaged between north and south observations. More details on these measurements are illustrated in appendix D.

2.1.3 Boreal forest sites

To verify how our modifications within MEB/Crocus impact the results obtained in previous studies at boreal forest observation sites, we compare the MEB/Crocus-new with MEB/Crocus-old at different sites used in previous studies.

Based on the study of Napoly et al. (2020), we use the data from the BERMS program (Boreal Ecosystem Research and Monitoring Sites) from Canada (53°N), Bartlett et al. (2006). This dataset, spanning from 1 November 1997 to 10 November 2010 has also been used in the latest snow model intercomparison project ESM-SnowMIP, and all the details of observation sites, forest parameters and forcing files are thoroughly described in Ménard et al. (2019) and Krinner et al. (2018).

Following Nousu et al. (2024), we also make use of data from two Finnish sites: Kenttärova (67°N) and Hyytiälä (61°N), where MEB/Crocus has been evaluated. Similarly, all the data and metadata required to run the subcanopy simulations are described in Nousu et al. (2024).

2.2 Models

To model snow under forest, we use the ISBA-MEB/Crocus model, shortly abbreviated into MEB/Crocus. ISBA is the module used in the SURFEX modelling platform (Masson et al., 2013) to simulate the surface and its interactions between the so-called “nature” (natural land surface) sub-grid patches and the atmosphere. MEB (Multi-Energy Balance model) is an option of ISBA that explicitly models vegetation canopy processes. Crocus (Lafaysse et al., 2025) is a detailed, physically-based snow

https://doi.org/10.5194/egusphere-2026-4137
Preprint. Discussion started: 1 September 2026

model originally developed for avalanche forecasting and usually applied at local to regional scales for a variety of applications (e.g., Morin et al., 2021; Dick et al., 2023; Réveillet et al., 2022; Roussel et al., 2024). More specifically, MEB/Crocus is a three-source model between vegetation, soil and snowpack. This configuration enables to model the coupling between a multi-layer soil and a multi-layer snowpack with a layer of canopy represented using the big-leaf approximation, whereby the entire vegetation is considered as a single effective leaf for mass and energy fluxes. All the equations for the energy balance are described in Boone et al. (2017).

Regarding mass fluxes, two reservoirs are used to model the forest water interception: a solid and a liquid interception reservoir (henceforth referred to as the liquid reservoir and solid reservoir).The model simulates the exchanges of mass between each of these two reservoirs, and the atmosphere and the ground or snow surface beneath the canopy. It also models any mass transfers (melting or refreezing) from one reservoir to the other. The fraction of the rainfall intercepted in the liquid reservoir is equal to the vegetation fraction non-covered by snow. Water from the liquid reservoir can either evaporate, refreeze (and be transferred into the solid reservoir), or drip to the surface beneath the forest canopy if it exceeds the maximum capacity. Snow from the solid reservoir can either sublimate, melt (and be transferred into the liquid reservoir), or unload to the surface beneath the forest canopy. The unloaded snow leaves the solid reservoir and increases the water equivalent of the snowpack beneath the forest canopy.

The following two sections describe in detail the formulations used to model the mass exchanges between the different compartments of MEB/Crocus. The main compartment of interest in our case is the solid reservoir, which will mostly be targeted by our modifications. We first describe the original version of the MEB/Crocus mass balance parametrizations for the solid reservoir (Sect. 2.2.1), then the modifications made to adapt it to the alpine climate (Sect. 2.2.2).

2.2.1 Original MEB/Crocus version (MEB/Crocus-old)

Interception of solid precipitation and maximum interception capacity

During snowfall or mixed precipitation events over forests, a certain proportion of snow precipitation is intercepted by vegetation. In the original MEB/Crocus model, the interception during a time step, I ($\mathrm{kg\,m^{-2}}$), depends on the initial amount of snow in the canopy, W_n ($\mathrm{kg\,m^{-2}}$), the density of the canopy, which is approximated in the model by LAI, the amount of snowfall, Ps ($\mathrm{kg\,m^{-2}\,s^{-1}}$), and the forcing wind speed, following Hedstrom and Pomeroy (1998):

$$I = (W_n^{max} - W_n)[1 - \exp(-k_n P_s \Delta t)] \tag{1}$$

Where W_n^{max} is the maximum load of the solid reservoir ($\mathrm{kg\,m^{-2}}$), depending on LAI:

$$W_n^{max} = S_n LAI \tag{2}$$

Where S_n is a coefficient that depends on fresh snow density and ranges from 4 to 6 $\mathrm{kg\,m^{-2}}$. k_n ($\mathrm{m^2\,kg^{-1}}$) is a coefficient that depends on LAI and wind speed (Boone et al., 2017, Eq.74) and ranges usually from 0.04 to 0.07 $\mathrm{m^2\,kg^{-1}}$

https://doi.org/10.5194/egusphere-2026-4137
Preprint. Discussion started: 1 September 2026

Melting and refreezing within the canopy

As previously stated, water melting from this solid reservoir flows into the liquid reservoir wherein it can be stored, drip or evaporate, while the solid part can be stored, unload or sublimate. Unloading increases the snow water equivalent of the snowpack directly, while a portion of the canopy drip (weighted by a snow fraction) can be intercepted by the snowpack and also increase the mass. Part of the water from the liquid reservoir can refreeze and add to the solid reservoir storage.

The formulation for melt and refreezing (Φ, $\mathrm{kg\,m^{-2}}$) is a classic degree-day using canopy air temperature (T_v, K) as follows:

$$\Phi = x_n k_\Phi (T_f - T_v) \tag{3}$$

Where k_Φ is equal to $5.56 * 10^{-6}\,\mathrm{kg\,m^{-2}\,s^{-1}\,K^{-1}}$, T_f is the fusion temperature for water: 273.15 K and $x_n = W_n / W_n^{max}$ is the fraction of snow-covered area. When $\Phi < 0$, the intercepted snow melts and the melted mass is transferred from the solid reservoir to the liquid reservoir. When $\Phi > 0$, the water in the liquid reservoir, if any, refreezes and the refrozen mass is integrated into the intercepted snow reservoir.

Unloading and characteristics of unloaded snow

Snow can also unload from branches and reach the snowpack on the ground. In MEB/Crocus, this unloading (U_n, $\mathrm{kg\,m^{-2}\,s^{-1}}$) is computed using the vegetation temperature (T_v), the forcing wind (U) and W_n based on Roesch et al. (2001):

$$U_n = -W_n \left(\frac{\max(0, T_v - T_v^U)}{C_T} + \frac{U}{C_V} \right) \tag{4}$$

with $C_T = 1.87 * 10^5\,\mathrm{K\,s^{-1}}$ and $C_V = 1.56 * 10^5\,\mathrm{m\,s^2}$ and $T_v^U = 270.15\,\mathrm{K}$ the temperature threshold for unloading. This parametrization differs from that described in the Boone et al. (2017), yet it has been employed since a long time in MEB.

Finally, the unloaded snow is incorporated into the total snowfall precipitation reaching the subcanopy as if it were fresh snow. It means that the properties of this new amount of snow within the detailed Crocus snow model (snow density, albedo, and snow grain characteristics) are computed in the same manner as for fresh snow, depending on air temperature and wind speed.

Figure 2 illustrates how this original version of MEB/Crocus (MEB/Crocus-old) performs in simulating SWE at Col de Porte in comparison to manual observations made under forests (green dots). Obviously, the model is unable to accurately reproduce the accumulation and melt of the subcanopy snowpack at this mid-altitude alpine site. It overestimates snow depth and fails to fit into the range of manual observations. These poor results in SWE and snow depth lead us to modify the parametrizations of canopy mass-balance processes within MEB.

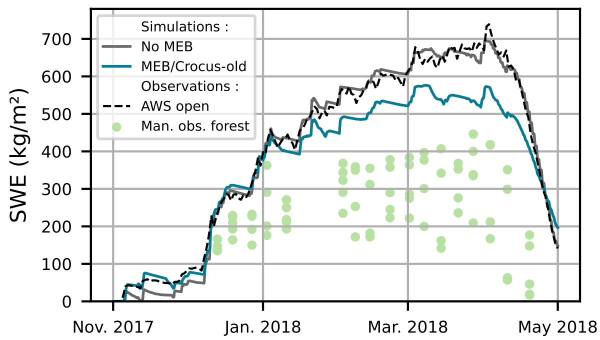

Figure 2. Comparison of open and under forest Snow Water Equivalent (SWE) observed and simulated at Col de Porte for the 2017-2018 winter season. No MEB is the open simulation, AWS open is the automatic observation in the open and Man. obs. forest the manual observations in the forest. Adapted from Vincent et al. (2018).

2.2.2 New MEB/Crocus version (MEB/Crocus-new)

In this section, we propose an enhanced formulation of some key processes of the snow-canopy interactions in MEB/Crocus, based on the comparison of MEB/Crocus to sub-canopy observations at Col de Porte (Vincent et al. (2018), Fig. 2), phenomenological observations and recent scientific literature (Lundquist et al., 2021; Roth and Nolin, 2019). The first objective of these enhancements is to improve the physical basis of the parameterizations used for snowfall interception and other mass fluxes affecting the solid reservoir. The second objective is to better represent the snowpack evolution under forest. Finally, these modifications are meant to be of general physical relevance and to preserve the performances of MEB/Crocus in other topographic and climatic contexts. For the rest of this article, this version is called MEB/Crocus-new.

To achieve these three objectives, we propose five modifications. They concern maximum interception capacity, interception, melt rate, unloading formulation and the properties of unloaded snow, and are described hereafter.

Maximum capacity of solid reservoir (*scaling* option)

Vincent et al. (2018) showed that the quantity of intercepted snow is largely underestimated by MEB/Crocus and that it is one of the main issues when simulating subcanopy snowpacks in an alpine climate. Typically, the maximum interception capacity of the original MEB/Crocus at Col de Porte (LAI = $4.5\,\mathrm{m}^2\,\mathrm{m}^{-2}$) following the formulation in Eq. (2) is about 15 to $20\,\mathrm{kg}\,\mathrm{m}^{-2}$, while observations suggest much higher load. The height of the boreal trees used to develop this formulation was between 10 to $20\,\mathrm{m}$ while in alpine forest, the tree tops can easily reach over $40\,\mathrm{m}$ height. In the new version of MEB/Crocus, a scaling factor is therefore introduced in order to take this effect into account, by increasing the snow holding capacity according to tree height: the forest LAI used to compute the maximum solid reservoir in MEB, is scaled according to the tree's height, compared to a reference height corresponding to the typical height of boreal forests where these processes have been parametrized:

$$LAI_{eff} = LAI \max\left(1, \frac{H}{H_{ref}}\right) \tag{5}$$

With LAI_{eff} the effective LAI now used in the solid reservoir parametrization, H the tree's height and H_{ref} the reference height (10 m). In order to account for the effect of size in energy fluxes, this effective LAI is also used to compute turbulent fluxes.

Enhanced snow interception at temperatures close to 0°C (*interception* option)

Vincent et al. (2018) (Fig. 2) showed that the original MEB/Crocus does not intercept enough snow compared to observations. Air temperature has a significant impact on the adhesion of the snow on branches: Lundquist et al. (2021) identifies this process as crucial for an accurate representation of snow interception while the original MEB/Crocus ignores it. Accounting for the effect of temperature on snow interception in MEB/Crocus is hence a promising way towards a more physical representation of interception and an increased amount of snow intercepted by trees.

As described in Lundquist et al. (2021) based on Schmidt and Gluns (1991), Kobayashi (1987) and Storck (2000), we use in the new version of MEB/Crocus the same formulation as Andreadis et al. (2009) to account for the fact that freshly fallen snow gets stickier at temperatures close to 0°C, especially from -3°C to +2°C. In this formulation, interception increases linearly between -3°C to 0°C with following boundary values:

$I_n = k_n^{min} P_s$ for $T_{air} \leq -3°C$

$I_n = k_n^{max} P_s$ for $T_{air} \geq -3°C$

with respectively $k_n^{min} = 0.6$ and $k_n^{max} = 1$, coherent with Lundquist et al. (2021) or Roth and Nolin (2019) . Note that this parameterization constitutes a complete change with respect to the original MEB/Crocus, with interception rate now independent of the maximum size for the solid reservoir and of precipitation rate. All interception in excess of the maximum size of the solid reservoir unloads directly.

Unloading (*unloading* option)

Following Lundquist et al. (2021), in the new MEB/Crocus we modify the original parametrization based on Roesch et al. (2001), by introducing two coefficients to reduce the amount of unloading and increase the time spent by snow on branches :

$$U_n = -W_n \left(M_T \frac{\max(0, T_v - T_v^U)}{C_T} + M_V \frac{U}{C_V}\right) \tag{6}$$

Where $M_T = M_V = 0.25$, $T_v^U = 273.15\,\mathrm{K}$ (values from Lundquist et al. (2021)). This function has already been widely used in land surface models, such as VISA (Niu and Yang, 2004) or CLM5.0 (Lawrence et al., 2019). More specifically, the vegetation temperature that reacts more rapidly to solar warming, is used here instead of the air temperature, to enhance the representation of the solar radiation effect on unloading observed at Col de Porte.

Melt of intercepted snow (*melt* option)

At Col de Porte, it has been observed that melt plays a key role in the mass balance of snow on trees (Vincent et al., 2018) and that it is underestimated by the original MEB/Crocus version. Based on Lundquist et al. (2021), we propose to modify the original degree-day coefficient from MEB/Crocus to reach values more commonly found in literature, so that now: $k_\Phi = 4.63 * 10^{-5}\,\mathrm{kg\,m^{-2}\,s^{-1}\,K^{-1}}$ ($4\,\mathrm{kg\,m^{-2}\,day^{-1}\,K^{-1}}$). This is a substantial modification as it corresponds to a multiplication by 10 of the original melt coefficient in MEB/Crocus.

Snow age of the unloaded snow (*aging* option)

In the original MEB/Crocus, the unloaded snow reaches the ground with characteristics of freshly fallen snow This does not fit alpine observations: in an alpine environment, the unloaded snow is significantly denser than fresh snow and has already experienced transformation (metamorphism, settling…) at the contact of trees. To be consistent with these observations, the unloaded snow in the new version of MEB/Crocus is added at the top of the underlying snowpack with specific properties corresponding to grains of melting snow with a density of $200\,\mathrm{kg\,m^{-2}}$ and a quite round form, characterized in Crocus by a sphericity of 0.9 and an optical diameter of 6*10-4 m. This adaptation is considered specific to mid-altitude alpine climate, as in other climatic contexts where unloading occurs predominantly through wind, this choice would be inappropriate.

2.3 Testing the sensitivity to top-canopy forcing conditions

In the classic multi-source bulk canopy approach used in MEB, the forcing reference level is designed to be above the top of the canopy, in accordance with the standard use of SURFEX/ISBA-MEB as a surface scheme coupled to an atmospheric model. However, for offline applications, common practices are to use as forcings either atmospheric model data (reanalyses for instance; e.g. Vernay et al. (2022)), or in-situ data acquired at nearby open sites, generally at screen-level (e.g., Ménard et al., 2019; Vincent et al., 2018), as observations above tall canopies are relatively rare. Most of the variables in the forcing (e.g. LW↓, SW↓, Rainf, Snowf, etc…) can reasonably be assumed to be very similar over trees and over nearby open areas. For air temperature and wind, however, this is not necessarily the case: forest characteristics, as well as the height above the ground, are crucial in shaping the above-canopy fields. However, an assessment of the sensitivity of subcanopy model simulations to the height/characteristics of the forcing data above forest canopies overlying snowpack has been so far, to the best of our knowledge, lacking. For instance, the data used in the ESM-SnowMIP project (Ménard et al., 2019) did not mention this possible issue.

Here, we address this knowledge gap by creating top-of-canopy forcing data for temperature and wind at Col de Porte, and exploring the sensitivity of the subcanopy snow simulation to this change with respect to reference forcing data derived from the in-situ observations at the open site.

https://doi.org/10.5194/egusphere-2026-4137
Preprint. Discussion started: 1 September 2026

For air temperature, we use the 32 m temperature sensor (T_{32}) as a top-canopy condition, as it is very close to the canopy top and overlies large branches directly exposed to the sun during daytime, similar to a top-canopy setting. We also explore how using other temperatures in place of top-canopy ones would affect the simulations, as top-canopy observations are usually not available. Typically, we test the impact of using:

- subcanopy 2 m air temperature observations (T_{for})
- an estimate of T_{32} derived from a multi-linear regression (T_{32reg}), using T_{air} at 2 m, LW↓, SW↓, and wind from the open site. This regression is notably meant to extend the 32 m temperature for years prior 2022 when the T_{32} measurement did not exist
- a proxy of top-canopy conditions based on the maximum between T_{open} and T_{for}: $T_{max} = \max(T_{open}, T_{for})$

The second component of the top-canopy forcing conditions that we investigate is wind, that is used to drive MEB/Crocus at 10 m above the canopy, hence in our case at 45 m above the ground surface. To estimate this top-of-canopy wind, we use a logarithmic extrapolation of the 10 m wind measured in open, as relevant for neutral atmospheric conditions. This extrapolation is based on the computation of the log-coefficient described in the right panel of Fig. 5 and depends on a roughness length that we call Z_{0f} (m, f for forcing) :

$$k_{wind}(Z_{0f}) = ln(Z_{top}/Z_{0f})/ln(Z_{ref}/Z_{0f}) \tag{7}$$

where $Ztop = 45\,\mathrm{m}$ represents the reference height for the wind forest forcing and $Z_{ref} = 10\,\mathrm{m}$ represents the reference height for the wind open forcing.

Within SURFEX (Masson et al., 2013), for an homogeneous zone covered by vegetation, $Z_{0f} = 0.13 * H_{veg}$ (Thom, 1971; Tanner and Pelton, 1960) where H_{veg} is the height of trees (m), hence $Z_{0f} = 4.5\,\mathrm{m}$ for the CdP forest. However, the terrain at Col de Porte is highly inhomogeneous, with open fields lying close to forest parcels. Furthermore the site is located at a pass with significant altitude differences between the site and neighboring mountains, making the terrain quite heterogeneous with respect to topography. Therefore the estimation of an appropriate Z_{0f} is complex. Therefore we will also explore the sensitivity of the subcanopy simulations to this parameter.

3 Results

3.1 Role of top-of-canopy conditions in shaping the sub-canopy snowpack

3.1.1 Role of air temperature

Differences between top-of-canopy, open and sub-canopy temperatures

https://doi.org/10.5194/egusphere-2026-4137
Preprint. Discussion started: 1 September 2026

Table 1. Metrics to compare forest air temperatures (T_{for}), open air temperature (T_{open}) and estimated top-of-canopy air temperatures (T_{max}, T_{32reg}), with top-of-canopy air temperature measurements (T_{32}). The winter corresponds to months between the 1st of November to the 30th of April (NDJFMA). The same metrics have been computed for peak winter period (DJF) and melt period (MA) and are available in supplementary material.

01/08/2022-02/08/2024	T_{open}	T_{32}	T_{32reg}	T_{max}	T_{for}
Mean (°C)	8	8.3	8.3	8.3	7.9
Winter Mean (NDJFMA) (°C)	2.4	2.6	2.6	2.5	2.4
Mean diurnal amplitude(°C)	7.5	6.4	6.6	6.9	5.6
RMSD (Ref: T_{32}, °C)	1.0	0	0.8	0.8	0.9

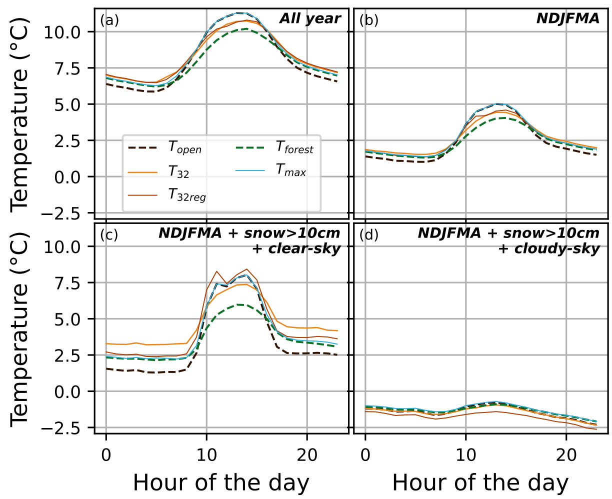

Figure 3. Diurnal cycles of air temperatures in the forest and open areas. (a) All the data available (01/11/2022 to 30/04/2024). (b) Only winter data (NDJFMA). (c) Winter data, snow depth > 10cm in open, 10% clearer days. (d) Winter data, snow depth > 10cm in open, 10% cloudier days. The selection of clear/cloudy day is based on the effective emissivity $e = LW\downarrow/(\sigma T^4)$, following Gouttevin et al. (2023)

.

Table 1 and Fig. 3 enable to synthesize the differences between top-of-canopy temperature conditions (assumed to be reasonably estimated via the T_{32} measure close to the top of the canopy crown) and open-field observations at screen level. These two-year statistics and diurnal cycles cover the period between 01/08/2022 and 02/08/2024. They also assess how well T_{for} and the two estimated proxies for top-of-canopy conditions: T_{max} (the max between T_{for} and T_{open}) and the linear regression T_{32reg}, can approximate T_{32}.

https://doi.org/10.5194/egusphere-2026-4137
Preprint. Discussion started: 1 September 2026

Neither T_{open} nor T_{for} diverge much from T_{32} on average: their mean difference with respect to T_{32} is lower or equal to 0.4 °C, with T_{for} being 0.4 °C cooler than T_{32} and T_{open} 0.3 °C cooler; these differences are reduced to 0.2 °C if considered only on an extended winter period (NDJFMA). However, the differences are stronger if the diurnal cycles are considered, as T_{open} and T_{for} have mean diurnal amplitudes that are, respectively, 1.1 °C higher and 0.8 °C lower than that of T_{32}. During the night, T_{open} is the coldest temperature, about 0.5 °C lower than T_{32}, and rising faster than the others in the morning so that, on average, it is the warmest temperature between 10:00 and 15:00, exceeding T_{32} by about 0.5 °C. Air temperatures are warmer than in the open at all heights within the forest at night, including at 32m, while during daytime they stay lower than T_{open}. During winter (Fig. 3 (b)), the diurnal amplitudes of all temperatures are reduced (4 °C during winter, instead of 7.5 °C for the whole year for T_{open}), but their relative behaviours remain the same. Fig. 3 (c) highlights that the main differences between all temperatures arise during clearer-sky days. On these days, the night/day differences are intensified: T_{open} is colder than T_{32} by almost 2 °C during the night and warmer by around 1 °C during the day. The selection of clear-sky days also highlights differences between T_{for} and T_{32}, T_{for} remaining cooler by around 1 °C during all day. All air temperatures are comparable during cloudy days. Both T_{32reg} and T_{max} estimates for top-of-canopy temperature have no mean bias with respect to T_{32} and have the same RMSD compared to T_{32}. The mean diurnal amplitude of T_{32reg} (6.6 °C) is closer to the mean diurnal amplitude of T_{32} (6.2 °C) than that of T_{max} (6.9 °C). Diurnal cycles show that T_{32reg} has a better fit with T_{32} on average over the whole period (Fig. 3 (a)), with almost no bias independently of the hour of the day while T_{max} underestimates it slightly during night (-0.4 °C at 6am) and overestimates it during day (+0.6 °C at 11am). These findings are confirmed for the winter data only (NDJFMA, Fig. 3 (b)). However, for clear-sky days, both T_{max} and T_{32reg} fail to fully reproduce the air temperature dynamics of T_{32}, with a clear underestimation during night (for T_{max}: -1 °C, for T_{32reg}: -0.8 °C at 3am) and overestimation during day (for T_{max}: +0.8 °C, for T_{32reg}: +1.6 °C at 11am). Nevertheless, T_{32reg} still has the lowest mean bias for clear days, with -0.3 °C compared to -0.6 °C for T_{max}.

Although T_{32reg} is a more accurate approximation of T_{32}, we confirm that T_{max} is an efficient proxy for T_{32}, with lower biases in absolute values, amplitudes, and lower RMSD than T_{open} and T_{for}. Using T_{max} is actually equivalent to using T_{for} during night-time hours and T_{open} during daytime, variables that are more frequently measured than top-of-canopy conditions. The use of T_{max} enables accounting both for the moderation of the nighttime temperature drop due to the thermal inertia of the forest, and for the increase in temperature due to radiation during daytime, both important characteristics of the top-canopy temperature. Therefore, in observation sites where top-of-tree measurements are unavailable, the T_{max} approximation could provide an interesting alternative to force models above the canopy.

For the following result sections of this article, all simulations will use T_{32reg} as it is the best proxy for T_{32} available during the whole study period, from 2016 to 2024.

Impact of top-of-canopy temperature on sub-canopy snowpack

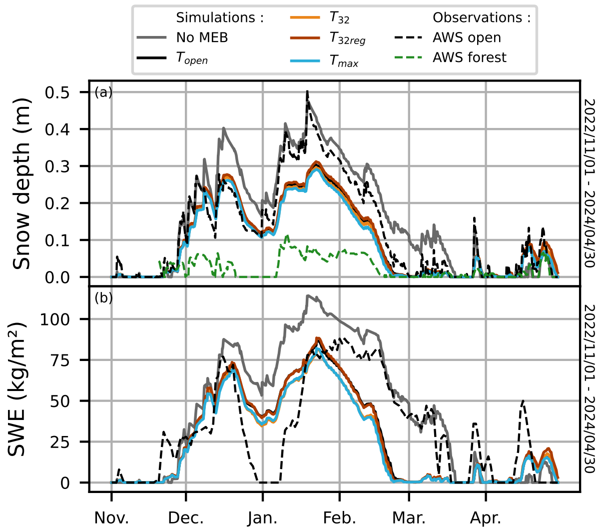

Figure 4. Average snow depth and SWE simulations and observations from 2022 to 2024. The solid lines represent simulations for different forcing air temperatures and No MEB is the open area simulation. AWS open is the automatic observation in the open area and AWS forest is the automatic observation in the forest. Year-by-year simulations are available in https://zenodo.org/records/21264265 (Pauze et al., 2026a).

We now evaluate how using top-of-canopy conditions instead of open-area nearby air temperature measurements (T_{open}), to force the MEB/Crocus forest-snow model, affects the simulation of the subcanopy snowpack at Col de Porte. Top-of-canopy conditions are either directly observed (T_{32}), or estimated through reasonable proxies: T_{max}, T_{32reg}. Simulations are performed accordingly over the 2022-23 and 2023-24 winter periods, which encompasses all observations and are run using MEB/Crocus-new.

The comparison between simulations with different air temperature forcings (Fig. 4) reveals almost no impact on the simulated snow depth below the forest. All simulations have very similar results and a RMSE of around $0.1\ \mathrm{m}$ compared to manual observation.

Independent of the specific year selected, the impact of air forcing temperature is negligible with a shortening of the snow period of maximum $2\ \mathrm{days}$ (observed in winter 2023-24) and no change in the peak snow depth. The minor sensitivity of the model to forcing air temperature changes is attributed to the fact that air temperature governs turbulent fluxes that are not major players in snowpack ablation compared to radiative effects (see Appendix B).

3.1.2 Role of wind

As described in the Data and methods section (Sect. 2), we use a logarithmic extrapolation to compute wind above the canopy, at $45\ \mathrm{m}$ above the ground surface. This logarithmic extrapolation depends uniquely on Z_{0f}. The effect of this coefficient on the estimated top-of-canopy wind is shown in Fig. 5, whereby this wind is compared with the forest wind at $2\ \mathrm{m}$ and the wind

https://doi.org/10.5194/egusphere-2026-4137
Preprint. Discussion started: 1 September 2026

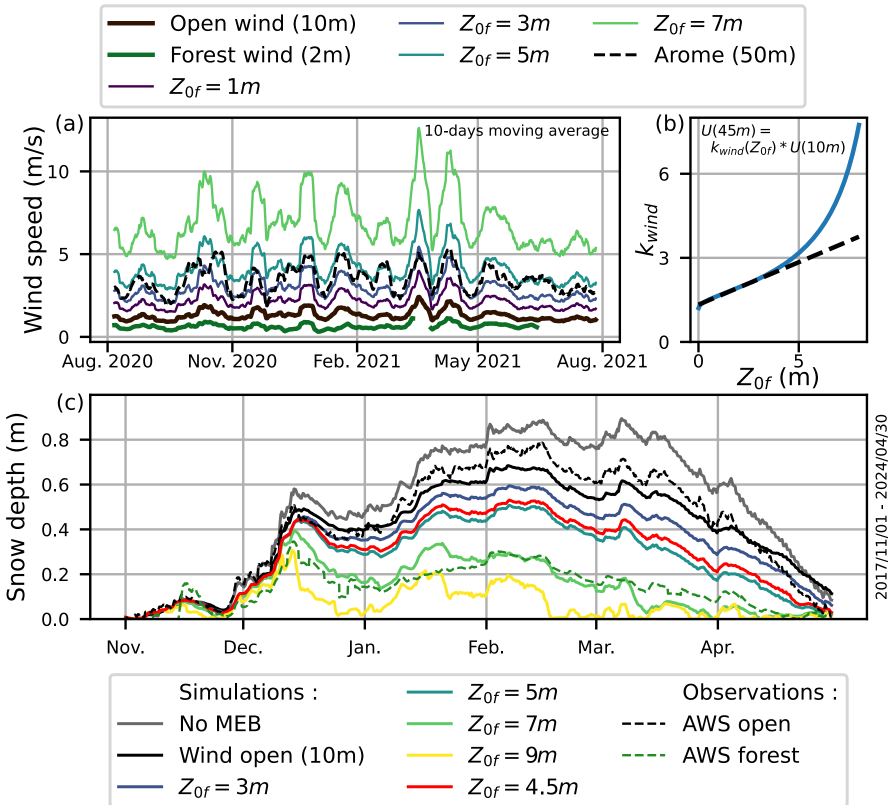

Figure 5. (a) Comparison between wind observations (thick lines), different log. extrapolations of the open wind at 10 m (fine lines), and the wind simulated by Arome at 50m above the surface. (b) Evolution of the extrapolation coefficient $k_{wind}(Z_{0f})$ as a function of Z0f. The behaviour is linear up to Z0f=4m and then theincrease is faster. (c) Effect on the snow depth simulation (average over 2017-2024) of the log. wind extrapolation to 10 m above the canopy with different Z0f. AWS open is the automatic observation in the open area and AWS forest is the automatic observation in the forest. Open wind (10m) is the simulation with MEB/Crocus using the open wind at 10m. Year-by-year simulations are available in https://zenodo.org/records/21264265 (Pauze et al., 2026a).

measured in the open at 10 m height. To gain some insight into a possible best-estimate for Z_{0f}, we also add to the comparison the wind computed at 50 m height by the Arome numerical weather prediction system, that runs operationally over France at 1.3 km spatial resolution (Seity et al., 2011). Arome takes into account the effects of subgrid topography and land-cover heterogeneity to compute an effective roughness length for wind. The effective roughness length given by AROME is 3.1m

With respect to just using an open-field observation of wind at 10 m above the ground surface, the use of the logarithmic extrapolation significantly increases the wind speed that forces the model at 10 m above the canopy (Fig. 5 (a)). This increase has a strong influence on the amount of snow on the ground below the canopy (Fig. 5 (c)), due to an enhancement of the turbulent fluxes: the higher the Z_{0f} parameter, the stronger the wind and therefore the turbulent exchanges that increase snow

https://doi.org/10.5194/egusphere-2026-4137
Preprint. Discussion started: 1 September 2026

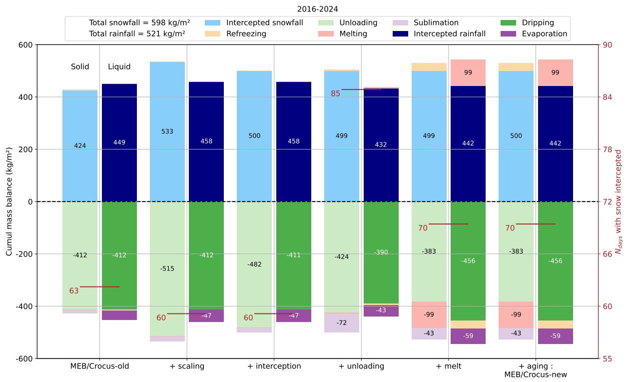

Figure 6. Effect of the different options of MEB/Crocus-new on the solid and liquid mass balance of the interception reservoir. Values are the average cumulative fluxes for winters (NDJFMA) between 2017 and 2024, regardless of snow cover on the ground. Horizontal red lines refer to the right y-axis and represent the number of days with snow in the solid reservoir. Year-by-year simulations are available in https://zenodo.org/records/21264265 (Pauze et al., 2026a).

loss on the ground through sublimation or energy available for melt (see Appendix B). For Z_{0f} values of $7\,\mathrm{m}$ or higher, the peak snow height is reduced by a factor more than 2 with respect to simulations forced with open-field $10\,\mathrm{m}$ wind speed. We note that this Z_{0f} parameter could be tuned to artificially fit the snow simulations to the observations (with a value $Z_{0f} = 7\,\mathrm{m}$, typically). Such an adjustment would significantly increase the sublimation and melting of the snowpack, leading to a temporal dynamics of the snowpack that does not correspond to the observational data. Indeed, there is a clear change in behaviour for Z_{0f} values greater than $5\,\mathrm{m}$: the decrease in snow depth from early February is too rapid compared to the data for $Z_{0f} = 7\,\mathrm{m}$ and even more so for $Z_{0f} = 9\,\mathrm{m}$. Thus, we choose to be consistent with SURFEX, whereby $Z_{0f} = 0.13 * H_{veg}$ resulting for Col de Porte in the value $Z_{0f} = 4.5\,\mathrm{m}$ An adjusted wind speed for a reference level above the canopy hence appears key in simulating the subcanopy snowpack energy and mass balances.

3.2 MEB/Crocus evaluation at Col de Porte

3.2.1 Effects of model modifications on canopy and sub-canopy mass balance

To adapt the MEB/Crocus scheme to alpine climate, we propose several modifications of MEB/Crocus interception, melt and discharge processes that are described in the methods section. In this section, we analyse the impact of these modifications on the subcanopy snowpack and interception mass balance.

Figure 6 shows the cumulative effects of the different options within MEB/Crocus-new on the different components of the canopy snow mass balance. For the next section, all the values will be the average over multiple snow seasons, ranging from the beginning of November to the end of April from 2016 to 2024.

MEB/Crocus-old intercepts a total of 424 $\mathrm{kg\,m^{-2}}$ (70% of total snowfall) of snow over the entire season with a maximum of 16 $\mathrm{kg\,m^{-2}}$ in the solid reservoir. The scaling option increases the maximum capacity of the solid reservoir in trees, thus increasing the snow interception up to a cumulative value of 533 $\mathrm{kg\,m^{-2}}$ over the season with a maximum of 30 $\mathrm{kg\,m^{-2}}$ in the solid reservoir. Using the scaling factor very slightly reduces canopy melt (from 1 $\mathrm{kg\,m^{-2}}$ to 0.3 $\mathrm{kg\,m^{-2}}$) and refreezing from liquid reservoir (from 3.5 $\mathrm{kg\,m^{-2}}$ to 1.4 $\mathrm{kg\,m^{-2}}$) but these values are negligible compared to the dripping from the liquid reservoir: 412 $\mathrm{kg\,m^{-2}}$. Because of the increase in interception, the unloading significantly increases from 412 $\mathrm{kg\,m^{-2}}$ to 515 $\mathrm{kg\,m^{-2}}$ while sublimation slightly increases from 13 $\mathrm{kg\,m^{-2}}$ to 18 $\mathrm{kg\,m^{-2}}$ meaning that almost all the additional snow intercepted via the scaling version is unloaded.

With the interception option, the intercepted snow is reduced by 33 $\mathrm{kg\,m^{-2}}$ to reach 500 $\mathrm{kg\,m^{-2}}$. This decrease reverberates directly to unloading with the same reduction, amounting to 482 $\mathrm{kg\,m^{-2}}$. The maximum of the solid reservoir is increased to 30 $\mathrm{kg\,m^{-2}}$ with this option.

Modifying the unloading parametrization does not impact the amount of snowfall intercepted or the melting of intercepted snow. By reducing the unloading from 482 to 424 $\mathrm{kg\,m^{-2}}$, it significantly modifies the number of days that snow spends in the solid reservoir from 60 days to 85 days, resulting in an increase of sublimation from 17 $\mathrm{kg\,m^{-2}}$ to 72 $\mathrm{kg\,m^{-2}}$.

Increasing substantially the melt rate does not change the amount of snowfall intercepted and the maximum in solid reservoir, but it significantly increases the melting from the solid reservoir, from 4 $\mathrm{kg\,m^{-2}}$ to 99 $\mathrm{kg\,m^{-2}}$ in seasonal totals, and the refreezing from 4 $\mathrm{kg\,m^{-2}}$ to 29 $\mathrm{kg\,m^{-2}}$. This increased melt reduces unloading (by 41 $\mathrm{kg\,m^{-2}}$) and sublimation (by 29 $\mathrm{kg\,m^{-2}}$) and adds to dripping (390 to 456/$\mathrm{m^2}$) and to a less extent, evaporation (43 to 59 $\mathrm{kg\,m^{-2}}$). This increase in the melt factor reduces the time with solid interception on the trees to 70 days, which explains the reduction in sublimation.

Resulting in a net increase in canopy losses (i.e. dripping, evaporation and sublimation), the two latter options have the most significant impact on the reduction of snow accumulation under forest. In contrast, the last (aging) option only modifies the properties of the unloaded snow but not the unloaded snow liquid water equivalent, thus it does not impact the mass balance in the trees or below.

3.2.2 Solid reservoir

We use the indirect interception observations from the 2019-2020 snow season (rectangles in forest site in Fig. 1) to evaluate the ability of MEB/Crocus-new and MEB/Crocus-old at simulating the intercepted snow dynamics.

This comparison is shown in the panel (a) of the Fig. 7 . Each measurement date is represented by a vertical line that characterizes the observed state of unloading, described by the observer. For 4 different boxes among the 8, the difference between the SWE in the open box and SWE in the subcanopy boxes is computed: these differences correspond to the colored dots (that refer to the left y-axis reading) with color indicative of LAI. This difference is equal to the amount of snow stored in the canopy when it is positive, and to the unloading, when it is negative. Observations of interception range from 0 to 40 $\mathrm{kg\,m^{-2}}$ with almost all snow intercepted for high LAI (yellow dot), e.g. the first snow event of November where the cumulative absolute snowfall is around 40 $\mathrm{kg\,m^{-2}}$ and the maximum interception measurements is 35 $\mathrm{kg\,m^{-2}}$. If we compare observations with the MEB/Crocus-old, it clearly underestimates the amount of intercepted snow, with a maximum of interception around 10 $\mathrm{kg\,m^{-2}}$.

https://doi.org/10.5194/egusphere-2026-4137
Preprint. Discussion started: 1 September 2026

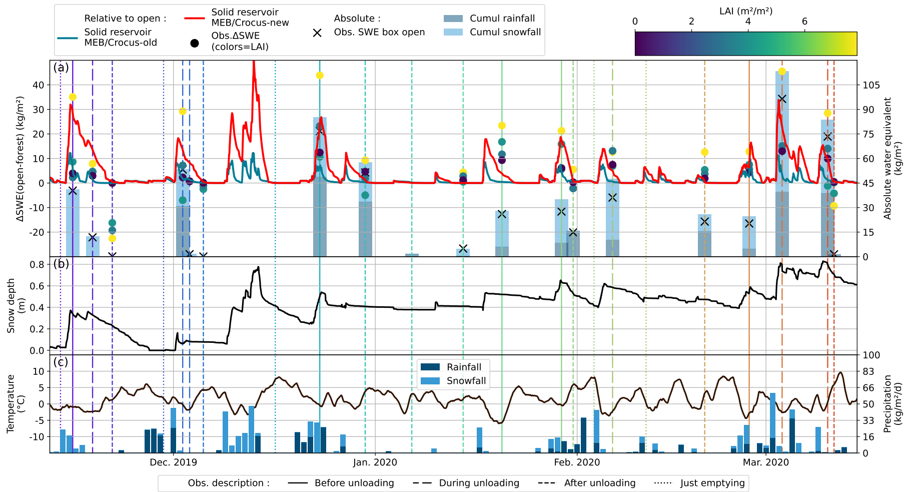

Figure 7. Indirect observations and simulations of the solid reservoir. The 28 vertical lines show the observation dates, with line style characterizing the unloading state as described by the observer. In (a), crosses show the measured SWE in open boxes and vertical bars the cumulative rainfall/snowfall since the last observation date; both refer to the right y-axis. The blue and red lines represent the simulated solid reservoir by the two model versions and refer to the right y-axis. The dots (colored by LAI) represent the difference between the open box and the forest ones, as a proxy for the solid reservoir (see Data and methods section, Sect. 2); they refer to the left y-axis. (b) represents the evolution of snow depth during the measurements period and (c) shows the open air temperature at 2m (1-day moving average) and daily precipitation.

The new version increases this maximum up to 50 $\mathrm{kg\,m^{-2}}$, which is a better fit to the observation. For almost all the events with measurements, the simulated solid reservoir from MEB/Crocus-new falls within the bounds provided by measurements with a variety of LAI values, most of the time between the green and yellow dots corresponding to a LAI around 4.5 $\mathrm{m^2\,m^{-2}}$, which is the value used in these simulations. The event of 20th of January is singular. The observation is classified as "before unloading", meaning that the observer noticed that no snow has unloaded yet. However, according to both versions of the model, more than half of the snow is already unloaded. Hence for this event, the simulated unloading is too fast both in MEB/Crocus-old and new.

3.2.3 Snow depth and SWE

In the Fig. 8, the impact of the modifications from MEB/Crocus-old to MEB/Crocus-new are illustrated for the total snow depth and the snow water equivalent below the canopy for the snow seasons between 2016 and 2022. For snow depth, the original version is around 0.2 m higher than the highest observations in forest and simulation is closer to open observations than to forested ones. Even if we consider that the open modelling ("No MEB") has a slight bias of excess snow and that this bias translates directly to forest simulations, we barely fit in the subcanopy observation distribution. By improving solid and liquid mass balance representation in the canopy according to literature recommendations and phenomenological observations,

https://doi.org/10.5194/egusphere-2026-4137
Preprint. Discussion started: 1 September 2026

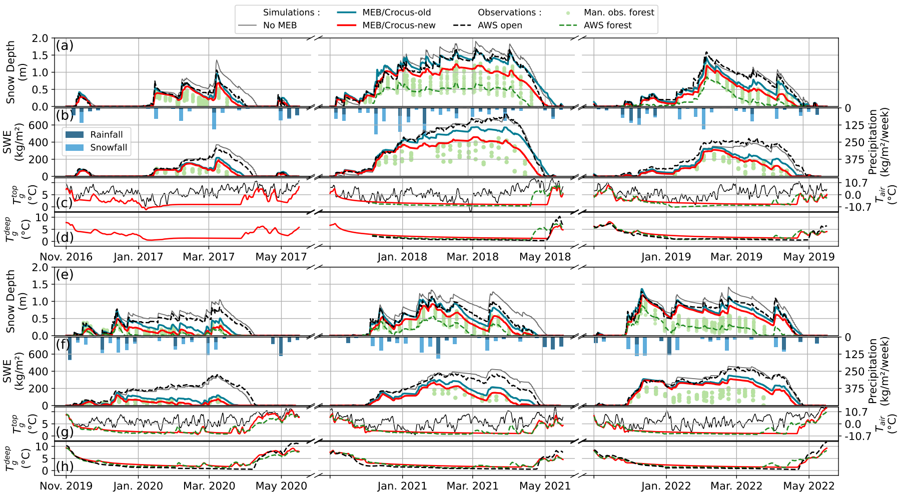

Figure 8. Snow depth and SWE observed and simulated at Col de Porte for 6 winter seasons (2016-2022). The simulations are represented by plain lines, with MEB/Crocus-old (2.2.1) in blue and MEB/Crocus-new (2.2.2) in red. The No MEB simulation is for open area without the activation of the MEB module. The green dots indicate the manual observations made in forest areas and the dashed lines represent automatic observations in the open area (black) and the forest (green). Two ground temperatures are displayed: T_{top}, corresponds to the top 5 centimetres of the soil, whereas T_{deep}, illustrates soil temperature evolution at a depth of 30 centimetres. To describe meteorological conditions, the observed air temperature (black thin line) and precipitation (blue bars) are also represented by referring to the right axis.

in MEB/Crocus-new, we clearly improve the representation of subcanopy snowpack. The RMSE of simulations compared to the sub-canopy snow poles is reduced from 0.58 m to 0.32 m for the 2017-2018 winter season and from 0.33 m to 0.21 m for all the winter seasons between 2016 and 2024. The mean bias compared to the poles is also reduced by roughly a factor 2, from 0.53 m to 0.25 m for the 2017-2018 winter season and from 0.27 m to 0.13 m for all the winter seasons between 2016 and 2024. Biases in modelling the subcanopy SWE are also significantly reduced, with a reduction of 40% of the season-averaged multiannual bias (from $115\,\mathrm{kg\,m^{-2}}$ to $70\,\mathrm{kg\,m^{-2}}$, amounting to 50% on the most snow-rich season 2017-18) and of 32% of RMSE (from $144\,\mathrm{kg\,m^{-2}}$ to $98\,\mathrm{kg\,m^{-2}}$).

Both absolute and relative improvements of the RMSE and mean bias are better for the 2017-2018 than for the whole period: among the winter seasons between 2016 and 2022, the 2017-2018 season is the snowiest. In fact, snowfall totals are close to the 30-yr climatological normal of the observed snow depth and SWE at Col de Porte, but recent winters within the 2010s and 2020s have been characterized by less snowfall.

Overall, the changes proposed in MEB/Crocus-new for the representation of the in-canopy mass-balance, significantly improve the representation of sub-canopy snow depth and SWE although values are generally along the upper envelope of the values measured at the stakes and still above the AWS estimates. In the next section, we take the opportunity of the availability of other ancillary observations at Col de Porte (see Sect. 2) to compare observed and simulated processes that affect the mass and energy balances of the snow under the forest.

https://doi.org/10.5194/egusphere-2026-4137
Preprint. Discussion started: 1 September 2026

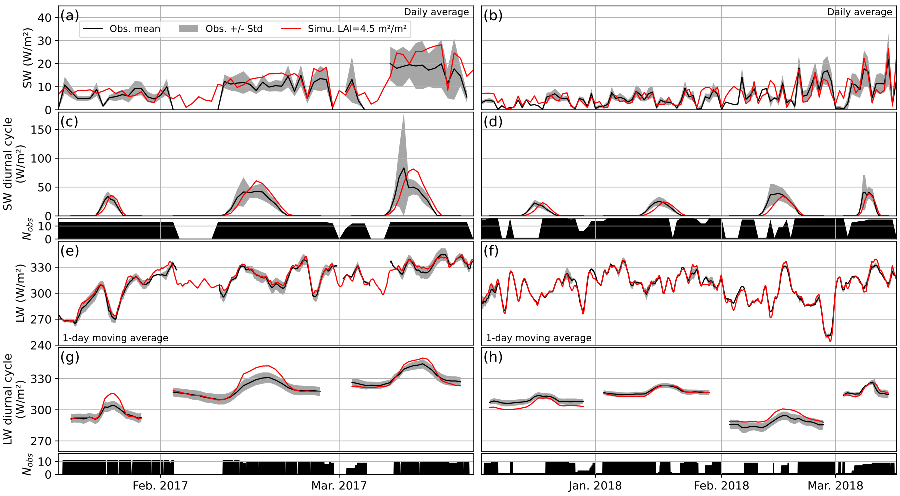

Figure 9. Comparison between subcanopy incoming radiation from radiometer observations (black line and grey envelop) and simulations for the average LAI at Col de Porte (red line) over winter seasons 2016-2017 and 2017-2018. (a, b, c, d) Daily average SW radiation and monthly diurnal cycles. (e, f, g, h) 1-day moving average of LW radiation and monthly diurnal cycles.

3.2.4 Evaluation against ancillary data at Col de Porte

More specifically, we here use various observations made in the forest site since the winter of 2016–2017 to evaluate the behaviour of MEB/Crocus-new in terms of subcanopy radiation, and canopy and sub-canopy air and soil temperatures. These observations come from the network of radiometers deployed for the 2 seasons of the SNOUF campaign to measure subcanopy SW↓ and LW↓ radiation, the forest AWS radiation observations, and more recent measurements of the canopy air, trees, branches and soil temperatures.

Subcanopy incoming radiation

During two winters, in 2016-2017 and 2017-2018, the SNOUF radiometers were placed at the surface of the snowpack in different places of the forest area (orange and yellow diamonds in forest site in Fig. 1). To compare these local observations with MEB/Crocus-new simulation for the global forest stand, we compute the weighted average and standard deviation of the observations, weighted by the representativity of LAI at each radiometer compared to the global LAI distribution as illustrated in Fig. A1 (b).

The temporal evolution and monthly diurnal cycles of these composite radiation fluxes are shown in Fig. 9 and compared to MEB/Crocus-new over the two snow seasons. The model tends to slightly overestimate the subcanopy incoming SW with a mean bias of $1.2\,\mathrm{W\,m^{-2}}$ and a RMSE of $5.4\,\mathrm{W\,m^{-2}}$ on daily average. While the model is most of the time within the standard deviation of the observations, more important errors occur during periods of fine weather (clear sky), such as from

https://doi.org/10.5194/egusphere-2026-4137
Preprint. Discussion started: 1 September 2026

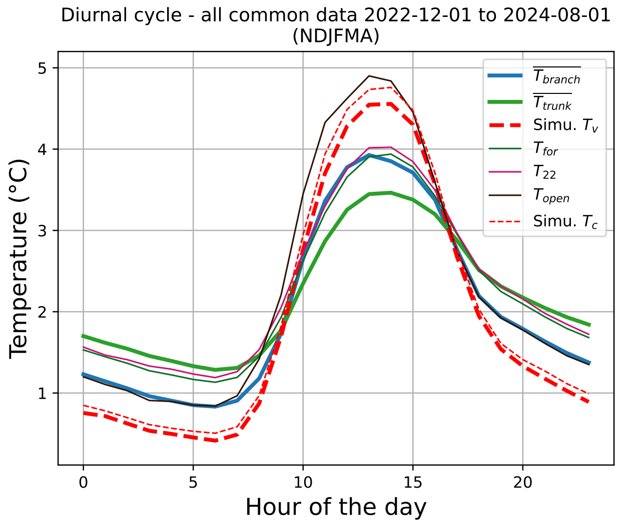

Figure 10. Diurnal cycles of vegetation temperatures (thick lines) and air temperatures (thin lines). For vegetation temperatures, observations are on branches and trunks and are averages of south and north observations (see Appendix D for more details). For air temperature, we compare T_{22}, T_{for} and T_{open} with simulated vegetation temperatures (T_V) and canopy air temperature (T_C).

late February to March 2017. In terms of diurnal cycle, the amplitude is in good agreement with observations for all months but the maximum is shifted by one hour in time. This is most likely due to the heterogeneity of the forest around the radiometers, with an east side more open than south and west.

The simulation of incoming LW radiation under the forest at Col de Porte is really satisfying, with almost no bias ($0.3\,\mathrm{W\,m^{-2}}$) and a RMSE of $5.9\,\mathrm{W\,m^{-2}}$ on daily averages. MEB/Crocus-new captures the temporal dynamics of subcanopy LW radiation and shows a good agreement with respect to the diurnal cycle as well. For the 2016-2017, it tends to overestimate the maximum LW during daytime but this bias does not appear in the 2017-2018 simulations.

Trunk, branches and air temperatures

To compute melt and unloading from the solid reservoir, MEB-Crocus uses the vegetation temperature, T_V. Therefore, this temperature directly impacts the solid/liquid ratio of unloading from the canopy, and the snow water equivalent on ground. Figure 10 compares the simulated vegetation temperatures of MEB/Crocus-new to observations on trunk and branches (green square in forest site in Fig. 1). The simulated vegetation temperature is closer to the branch temperature than to the trunk temperature. This behaviour seems to be consistent since MEB represents only one bulk canopy layer, with a thermal inertia representing all vegetation elements (from needles to branches and trunks) and energy exchanges both with the open air and intra-canopy environment, while the trunk is mostly exposed to intra-canopy conditions. More precisely, the mean simulated vegetation temperature is equal to the mean temperature of the branches, while the model underestimates trunk temperatures by

https://doi.org/10.5194/egusphere-2026-4137
Preprint. Discussion started: 1 September 2026

0.2 °C. Although mean model biases are hence very weak, the diurnal cycles on Fig. 7 reveal a clear difference between daytime and nighttime model behaviors, with the model overestimating vegetation temperature during daytime and underestimating it during nighttime. If we define night as hours between 6pm and 6am, mean vegetation temperature during night is 5.6 °C for MEB/Crocus-newsimulations, while it is 6 °C for branches observations and 6.6 °C for trunk observations. During the day, the model mean is 8.8 °C, while branches have a mean temperature of 8.2 °C and trunk 8 °C. We also hypothesize that this results from the observed branches and trunk being well within the lower canopy, at locations rather sheltered from the upper-canopy air or the open air, thus exhibiting dampened diurnal air temperature variations, while the modelled bulk vegetation layer is in part directly exposed to open air top-of-canopy conditions resulting in higher thermal amplitudes.

MEB-Crocus is using an internal canopy air temperature, T_C, to compute the surface energy balance through aerodynamic resistances coupling ground, vegetation and atmosphere. Even if this model variable is conceptual, it is still interesting to compare it with observations of air temperatures acquired in the forest : T_{for} (T_{air} at 2 m from the ground in the forest), T_{22}. The open air temperature at 2 m appears also in Fig. 10. A different behavior is observed between day-time and night-time conditions, with a cold bias for simulated T_C during the night and the opposite during the day. Furthermore, as we ascend through the canopy, the simulated temperature T_C becomes increasingly colder in comparison to observational data. The mean bias for T_{for} is -0.1 °C, while for T_{22}, it is -0.25 °C.

Trunk, branches and air temperatures

Soil temperatures, presented in Fig. 8, are relevant variables to evaluate the energy balance of the ground in MEB/Crocus. During the snow-covered period, the model demonstrates a high level of agreement between measured and simulated temperatures at all depths (between 2.5 cm and 60 cm). During the six winters studied between 2016 and 2022, the observed ground temperature is very stable due to snowpack insulation. Thus, it was observed that the simulated temperatures closely matched the measured ones, showing no bias at any depth. The disparities between modeled and observed ground temperatures become evident when there is a discrepancy between the observed melt-out date and the simulated one. Typically, for 2019, the first snow-free event is not captured by the model ; therefore, the temperature rise at the beginning of April is not modeled. However, as soon as snow disappears, all simulated ground temperatures closely align back with observations.

3.3 Validation at boreal sites

In this final Results section, we verify that the modifications presented in this article do not significantly impact the previous validations of MEB/Crocus, performed on other sites, especially boreal sites. Hence, average snow depth simulation results with MEB/Crocus-new and MEB/Crocus-old for the three BERMS (Canada) sites: OAS, OBS and OJP ; and the two Finnish sites: Kenttärova and Hyytiälä, are shown in Fig. 11.

MEB/Crocus-new demonstrates a marginal improvement in model performances at the BERMS sites, as it exhibits a reduction in RMSE for snow depth at the three sites when compared to automatic forest snow height observations. For the winter season (NDJFM), the RMSE decreased from 0.16m (original) to 0.13 m (final) for OAS, from 0.09 m to 0.06 m for OBS, and

https://doi.org/10.5194/egusphere-2026-4137
Preprint. Discussion started: 1 September 2026

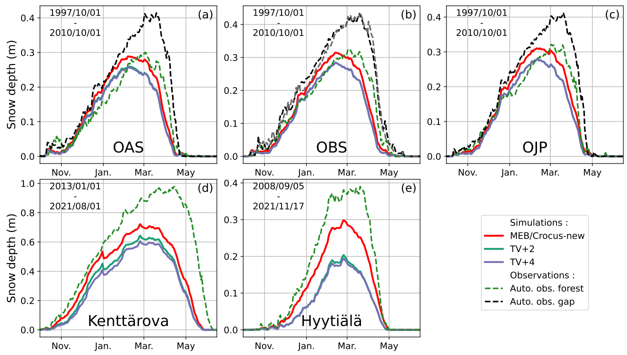

Figure 11. Average snow depth at the boreal sites. Solid lines represent simulations and dotted lines observations. Gap observations are observations in open areas. For the OBS site, two gap observations are available with close results, one is in grey and the other is in black. The No MEB simulation is for the open area without the activation of the MEB module. Year-by-year simulations are available in https://zenodo.org/records/21264265 (Pauze et al., 2026a).

from 0.11 m to 0.07 m for OJP. These improvements are also discernible on the temporal evolution of snow shown in Fig. 11 : MEB/Crocus-new more accurately captures the accumulation period, without unduly degrading the melt period. MEB/Crocus-new is still unable to accurately represent the time of maximum snow accumulation. However, it should be noted that this bias is not specific to MEB/Crocus-new, as both the open simulation and original version also fail to reproduce this timing.

For the two Finnish sites, MEB/Crocus-new exhibits a very marginal deterioration in the simulation behavior, with RMSE increasing by 0.01 to 0.02 m, from 0.13 m (MEB/Crocus-old) to 0.14 m (MEB/Crocus-new) for Kenttärova and from 0.08 m to 0.1 m for Hyytiälä. As demonstrated in Fig. 11, this decline in performance is primarily attributable to a small decrease in accumulation, which predominantly affects the maximum accumulation and does not alter the melt-out date between the two versions of MEB/Crocus. Moreover, the comparison with subcanopy snow depth observations for these two sites appears to be challenging, as even the open simulation struggles to reproduce the observed behavior (particularly at Kenntärova), suggesting that the bias may originate from the precipitation or other terms of the meteorological forcing.

In summary, for boreal sites, MEB/Crocus-new demonstrates comparable or improved performance. This provides confidence in the relevance of the parametrization adaptations and suggests that they are not over-calibrated for Col de Porte.

4 Discussion

4.1 On the relevance on a maximal snow interception capacity

As demonstrated in the works of Lundquist et al. (2021) and Cebulski and Pomeroy (2025), there is no empirical evidence that validates the hypothesis of a maximum snow interception capacity. This assessment has been verified in MEB/Crocus-new: the maximal capacity encoded in the model has no further impact on interception or unloading and is simply a maximum threshold of around 75 $\mathrm{kg\,m^{-2}}$. As shown in Fig. 7, this threshold is never reached for the 2019-2020 winter simulation, nor

https://doi.org/10.5194/egusphere-2026-4137
Preprint. Discussion started: 1 September 2026

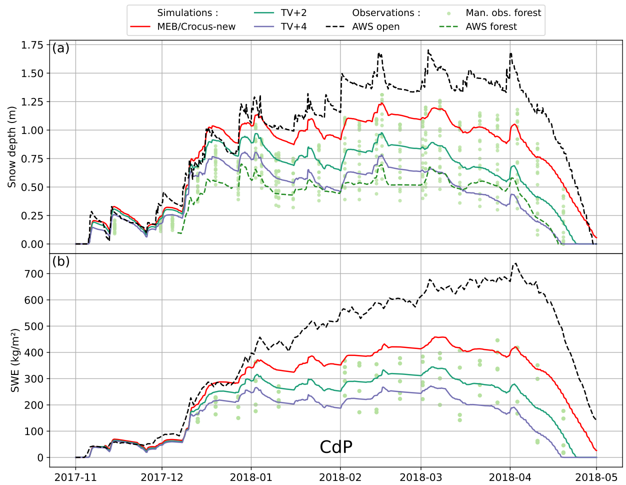

Figure 12. Simulated and observed snow depth and SWE at Col de Porte over winter 2017-2018. The simulations show the model sensitivity to the TV+2/TV+4 setup compared to manual observations (green dots) and automatic observations in the open area and the forest. Results for boreal sites are available in C. All the years between 2016 and 2024 are available in https://zenodo.org/records/21264265 (Pauze et al., 2026a).

for the seven other winters from 2016-2024. This finding lends further support to the hypothesis that the model does not necessitate a maximum solid reservoir to accurately simulate the snow mass balance in trees. Furthermore, manual interception measurements were conducted during the 2025-2026 winter season at Col de Porte, involving the manual removal of snow from branches and the weighing of the corresponding snow amount (data available in ref:data repository). These observations demonstrated that the effective length of interception, defined as the length of the branch observed from the sky, can be divided by three when the branch is loaded with snow, with a deflection of $2\,\mathrm{m}$ for a four-meter branch. This result, combined with the observations from Schmidt and Pomeroy (1990) and Bründl et al. (1999), which demonstrate relationships between branches bending and vegetation temperature, make this concept of maximum interception not clear as soon as this value does not depend on temperature. We therefore find that our results corroborate the conclusions of Lundquist et al. (2021) about the frail relevance of the concept of maximum interception capacity.

4.2 Representation of the vegetation temperature and implications for determining canopy snow melt

MEB/Crocus-new demonstrates an enhanced representation of snow under forest at Col de Porte, without compromising the results obtained from simulation at boreal forest observation sites. Nevertheless, there is still potential for the simulations at Col de Porte to be improved. Indeed, MEB/Crocus-new continues to overestimate snow depth in comparison to the manual observations (Fig. 8), with simulated values that are comparable to the highest observed values in the quite heterogeneous forest stand. These correspond to LAI values of around 0 to $1\,\mathrm{m^2\,m^{-2}}$, despite the LAI of the simulation being $4.5\,\mathrm{m^2\,m^{-2}}$. For the 2021-2022 season, the simulation does not even meet the observations distribution: the model bias develops during

https://doi.org/10.5194/egusphere-2026-4137
Preprint. Discussion started: 1 September 2026

one early precipitation event in Dec 2021, and is then constant over the winter season. It does not appear to be attributable to precipitation errors in the meteorological forcing, as the simulation for the open area accurately matches the open observation (and representativity errors in the open observations are minor due to very little topography at the site and marginal snow transport by wind). This leads us to try to elucidate this bias at the beginning of the season, which is likely attributable to physical processes not sufficiently well represented in MEB/Crocus.

Following the findings of Vincent et al. (2018), our primary modeling target in this study was to enhance the melt of snow within the canopy at Col de Porte, as this seemed a prerequisite to better reproduce the subcanopy snowpack dynamics and associated processes at this site. In Crocus/MEB-new, the degree-day factor for the melt in the solid reservoir has been increased to values that are consistent with those reported in the literature; so that a further increase does not seem justified. The temperature of vegetation employed in the parametrization of the melt of the intercepted snow may however present a cold bias for a number of hours (Fig. 10) in comparison to the observed vegetation temperatures. Furthermore, these observations of vegetation temperature may not be representative of the branches and needle temperatures triggering the melt of the intercepted snow. Indeed, they were measured on a medium-sized tree at a height of two meters above the ground, that is to say in a lower canopy setting, quite sheltered from direct solar radiations from the higher surrounding canopy. So, they may underestimate the temperature of higher canopy elements; more exposed to direct sunlight on clear-sky melt events. As demonstrated in literature (Gouttevin et al., 2015; Webster et al., 2016b), the temperature of the canopy is misrepresented by one-layered canopy models that cannot capture the different thermal behaviours of inner-canopy and upper-canopy environments. Moreover, in MEB/Crocus, the vegetation temperature is a synthetic temperature for vegetation and for liquid and solid water intercepted. This effective temperature can not represent the different energy processes from the top of the trees to the bottom, from needles to trunk or from vegetation to water. For instance, the top of the canopy is more connected to the atmosphere and the vegetation temperature follows more the open air temperature while in the understory, trees damps atmosphere variation (Fig. 3). It has been determined that the temperature of vegetation can differ from -5 °C to +5 °C from the air temperature in gaps during a clear-sky day at 12:00, depending on the insolation of trees (Webster et al., 2017). Therefore, it can be hypothesized that the temperature of the top of the vegetation could be a few degrees higher during daytime in sunny conditions, than the actual simulated vegetation temperature, or observed vegetation temperature in the inner-canopy, leading to enhanced melting when solid interception is present.

Following this hypothesis, numerical tests were conducted in which Tv was increased by 2 °C (TV+2) and 4 °C (TV+4), exclusively within the parametrization employed to compute melt of the intercepted snow. As illustrated in Fig. 12 for CdP (results for boreal sites are available in appendix C), this increase in vegetation temperature enables an earlier melt and directly impacts the snow dynamics in the accumulation period. It drastically reduces the SWE bias, from 70 $\mathrm{kg\,m^{-2}}$ to 30 $\mathrm{kg\,m^{-2}}$ for TV+2, and to 0 $\mathrm{kg\,m^{-2}}$ for TV+4. These improvements can be attributed to changes in the partitioning between unloading and dripping, as evidenced by the following values: for MEB/Crocus-new, 383 $\mathrm{kg\,m^{-2}}$ unloads and 456 $\mathrm{kg\,m^{-2}}$ drips (Fig. 6); while for TV+2 (resp. TV+4), 287 $\mathrm{kg\,m^{-2}}$ (resp. 190 $\mathrm{kg\,m^{-2}}$) unloads and 571 $\mathrm{kg\,m^{-2}}$ (resp. 686 $\mathrm{kg\,m^{-2}}$) drips. In all these simulations, the quantity of water reaching the ground remains relatively constant. However, the ratio of liquid discharge over total discharge (dripping plus unloading) is strongly affected by our TV+2/TV+4 modifications, with values increasing

https://doi.org/10.5194/egusphere-2026-4137
Preprint. Discussion started: 1 September 2026

from 54% for MEB/Crocus-new to 67% for TV+2 and 78% for TV+4. The following section (Sect. 4.3) is dedicated to the development of this question. Finally, our TV+2/TV+4 setups provide promising insights for improving the simulations, but also highlights the need for more detailed observations of vegetation temperatures to consolidate our hypothesis and adopt appropriate modeling choices. These further investigations and refinements appear necessary to accurately capture the subcanopy snowpack dynamics in temperate mountain environments where mid-winter melt events and interception melt are frequent.

4.3 Distinction between solid and liquid discharge is the next observational challenge

Eventually, the distinction between liquid and solid discharge in the models is currently not clearly constrained by observations.

As asserted by Storck et al. (2002), the phenomena of meltwater drip and unloading nearly always occur simultaneously, thereby rendering the precise observation of meltwater dripping alone a complex task. As stated in Lundquist et al. (2021), the correlation between unloaded snow and the dripping of liquid water has been documented in numerous observational studies. However, these studies show that the proportion of the total solid reservoir melting and dripping as liquid water varies significantly, ranging from 5% to 60% (Kittredge, 1953; Satterlund and Haupt, 1967; Storck, 2000). A recent experimental study (Cebulski and Pomeroy, 2026) with in situ observations from a needleleaf forest in the Canadian Rockies has demonstrated that the unloading-to-melt ratio increases in a linear manner with canopy snow load, ranging from 1 to 5. This indicates that the melt constitutes between 100% and 20% of the unloaded snow, and provides a rare insight into a possible explanatory mechanism for the wide range of the previously cited observations for this ratio, of high interest for modelling. Alternatively, using cut-tree experiments and weighing lysimeters around single trees, Storck et al. (2002)) measured the partitioning between drip and unloading on two events over three years of observations, identifying a constant ratio of mass release to meltwater drip of 0.4. This result is presented as a first hypothesis of partitioning and suggests that meltwater is a trigger for solid unloading.

In models, parameterizations are known to be widely spread, as synthesised in Lundquist et al. (2021): the unloaded snow could be assumed to be all solid (Essery, 2015; Mazzotti et al., 2020a) or a mix between liquid and solid with constant proportion (40% for Andreadis et al. (2009)) or variable as in MEB/Crocus. This wide range of values demonstrates the challenges associated with better constraining the amount of drip through observations and proposing appropriate explanatory mechanisms and parameterizations for models.

At Col de Porte, the indirect interception measurements presented above, do not enable to distinguish between the part of the water equivalent measured in the boxes due to liquid discharge (dripping), from that resulting from (solid) unloading. This is because snow can melt and liquid water can refreeze in the boxes. Visual observations at this site suggest that dripping plays a key role in the process of snowmelt ablation from trees. This is evidenced by observations of substantial drip events, which resemble rain falling beneath the forest canopy, when trees are loaded with snow. It appears that this melt water functions as a lubricant during the unloading process. To date, none of these processes have been subjected to quantification, and it is evident that more complex observational setups are required in order to distinguish their different contributions. Their observation could improve the parameterizations of dripping and unloading into MEB/Crocus, and possibly help reduce snow on the ground by increasing dripping from trees. As the physical processes involved have not been clearly identified, the quantification of liquid versus solid ablation of mass from trees poses a challenge with significant potential implications for hydrology.

https://doi.org/10.5194/egusphere-2026-4137
Preprint. Discussion started: 1 September 2026

5 Conclusions

The present study was motivated by the fact that the MEB/Crocus model, originally developed to capture forest-snow interactions in high-latitude settings, performs poorly at the mid-altitude Alpine site Col de Porte and in intercomparison on dense alpine forest, suggesting it could possibly be the case for other Alpine sites. Preliminary tests were pointing towards inadequate interception parameterizations. Five modifications for the parameterization of intercepted snow and associated fluxes were therefore proposed to enhance the physical representation of the various processes that impact accumulation and ablation of intercepted snow. In detail, the interception rate was modified to account for the increasing adhesion of snow on branches for air temperature around 0°C. The unloading parametrisation was revised to a more physical representation based on vegetation temperature and wind speed. The LAI was rescaled for the estimation of the maximum solid reservoir, to take into account the height of the trees. The degree-day coefficient governing the solid interception melt was modified to correspond to values described in the literature. Finally, the unloaded snow was considered as aged snow.

These modifications reduced the simulation errors at Col de Porte compared to the observations in terms of both SWE and snow depth. The indirect interception observations dataset also enabled us to evaluate these improvements at the process scale, by demonstrating a more coherent snowfall interception amount and timing of unloading. The two versions of the model were also tested and compared at two boreal sites, in Canada and Finland, and the new version demonstrated convincing results in the representation of the snow under forest for these sites.

Further investigations were conducted to try to explain the remaining positive bias in SWE and snow depth for the simulated subcanopy snowpack at Col de Porte. Encouraging results were obtained by increasing the vegetation temperatures used in the melt parametrisation, thus favouring drip over solid unloading. This is justified by the fact that the temperature of leaves and needles in contact with intercepted snow and exposed to the sun at the top and edges of the canopy, may differ substantially from the temperature of the bulk trunk and branches layer in the model, as a result of the faster heating of these leaves and needles by radiation.

A key question remains about the partitioning between liquid and solid unloading, as this process is particularly difficult to distinguish in observations and exerts a key control on the subcanopy snowpack. Finally, the improvements made to the MEB/Crocus model are promising to deliver a better representation of snow and forest interactions, of benefit for hydrological modeling in Alpine context.

Code availability. The Crocus snowpack model is developed within the opensource SURFEX project with CeCILL-C 1.0 license (https://cecill.info/licences/Licence_CeCILL-C_V1-en.html, last access 6 July 2026). The source code of the version referred to in this work can be accessed freely on https://doi.org/10.5281/zenodo.21263777 (Pauze et al., 2026b). The SURFEX code will evolve after sub-mission and publication. The most up-to-date stable version of Crocus can be accessed through the branch cen of the SURFEX git repository (https://github.com/UMR-CNRM/SURFEX_CEN, last access 7 July 2026). The modified version used in this article is tagged as forest-PauzeGMD_2026.

https://doi.org/10.5194/egusphere-2026-4137
Preprint. Discussion started: 1 September 2026

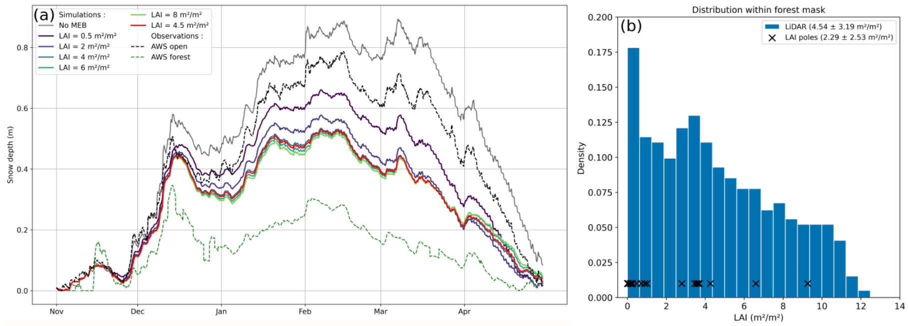

Figure A1. (a) Average observations and simulations for the 7 winter seasons between 2017 and 2024. Colored simulations describe the sensitivity of MEB/Crocus to LAI, and No MEB is the open area simulation. Year-by-year simulations are available in https://zenodo.org/records/21264265 (Pauze et al., 2026a). (b) LAI distribution derived from the LiDAR HD dataset. Crosses represent the LAI for the 18 poles where manual snow depth and SWE observations are made under the forest.

For more information on the installation and use of the SURFEX code, please refer to the Data and Code availability section of Lafaysse et al. (2025).

Data availability. All the data and figures of this article are available at https://zenodo.org/records/21264265 (Pauze et al., 2026a) under the terms and conditions of the Creative Commons Attribution 4.0 International license.

All the data used in this study are available in netcdf format. It includes all the simulation files and the forcing and namelist associated with each simulation, with a small description for each specific simulation. All the observations from the different sites presented in this article are also accessible.

An xlsx file containing manual observations of interception based on direct measurements of all snow accumulated on a small tree on two dates is also available in the data repository. This file is accompanied by pictures and a readme file that provides a detailed description of the methods used to conduct these observations.

All the figures are available in the repository. For the figures that represents average over multiple snow seasons, year-by-year figures are available in the repository.

Appendix A: LAI measurements and model sensitivity at Col de Porte

To simulate sub-canopy snow at Col de Porte, the MEB/Crocus model is using a set of parameters to describe the forest. The main parameters are the LAI (Leaf Area Index) which represents leaf density ($\mathrm{m^2\,m^{-2}}$) and H_{veg}, the tree height (m), that modulate the roughness length (Z_0, m) and subsequently the turbulent exchanges between the surface, the intra-canopy air and the above-lying atmosphere. The tree height is supposed to be fixed to 35 m, which is the average for the main trees at Col de Porte.

https://doi.org/10.5194/egusphere-2026-4137
Preprint. Discussion started: 1 September 2026

To derive LAI values at Col de Porte, we used the LiDAR HD dataset (https://geoservices.ign.fr/lidarhd, last access 10/07/2026) over the Col de Porte area, to derive 2-m scale LAI data using the library LidR (Roussel et al., 2020) based on the method published by Bouvier et al. (2015) et Kamoske et al. (2019). In order to reduce the effect of canopy absorption on the lidar beam, only data acquired at a zenithal angle of 10 ° or less were used. The initial LiDAR point cloud has an average density of 44 $\mathrm{pointsm^{-2}}$, with the zenithal angle filtering, we obtain a resolution of 15 $\mathrm{pointsm^{-2}}$.

For the Col de Porte forest site, the LAI distribution computed using LiDAR measurements is shown in Fig. A1 (b) : it ranges from 0 to around 12 $\mathrm{m^2\,m^{-2}}$ and poles where we measured snow have LAI mostly below 5 $\mathrm{m^2\,m^{-2}}$. Stand-average LAI is 4.5 $\mathrm{m^2\,m^{-2}}$ with a standard deviation of 3.2 $\mathrm{m^2\,m^{-2}}$. This distribution is used to weight radiometers representativity when computed average and standard deviation : radiometers are splitted in 5 LAI categories (0-2, 2-4, 4-6, 6-8, 8-10, >10 $\mathrm{m^2\,m^{-2}}$) and averages and standard deviations are weighted using the proportion of each category in the LAI distribution. The Fig. A1 (a) shows that the snow depth simulated by MEB/Crocus is sensitive to low LAI variation but reaches a plateau for LAI above 4 $\mathrm{m^2\,m^{-2}}$ with almost no difference in behaviour between 4 $\mathrm{m^2\,m^{-2}}$ to 10 $\mathrm{m^2\,m^{-2}}$. The main impact of LAI variation is for accumulation and melt period : with a low LAI, accumulation on the ground increases as interception decreases. However, the melt rate is enhanced at the end of the snow season due to higher solar radiation and this compensates the excess of snow accumulation ,bringing to a melt-out date similar for all LAI values. At the timing of peak snow accumulation, the difference in subcanopy snow height between the simulation with LAI close to the lowest and highest bounds (0.5 and 10 $\mathrm{m^2\,m^{-2}}$, resp) is, on average, around 0.3 m, of accumulation under forest which is consistent with the typical spread of observations.

For all the simulations presented the LAI used is of 4.5 $\mathrm{m^2\,m^{-2}}$.

Appendix B: Energy balance sensitivity to Z_{0f}

Appendix C: Model sensitivity to change in threshold temperature for melt of solid reservoir

Appendix D: Treatment of vegetation temperature

Author contributions. AaB, IG and YL designed the original research project. TP carried out most of the research and chose its orientations. TP and AxB modified the code and performed the model evaluations with scientific contributions of AaB, IG, YL and ML. TP was responsible for writing the article, with significant contributions from AaB, IG, and YL and input from all the authors. MF supported the simulation workflow and other technical aspects. ELG maintained the observatory site and forest instrumentation.

Competing interests. The authors declare that they have no conflict of interest.

https://doi.org/10.5194/egusphere-2026-4137
Preprint. Discussion started: 1 September 2026

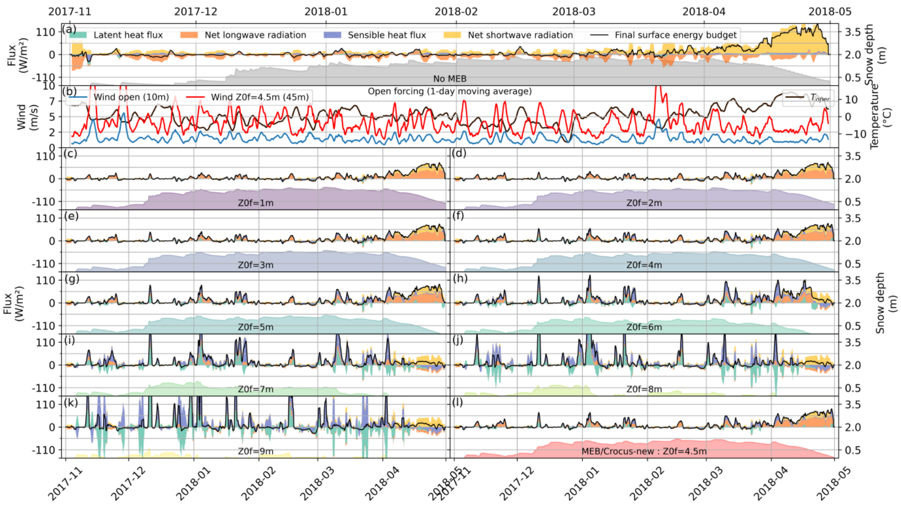

Figure B1. Surface energy balance of the ground snowpack depending on the Z_{0f} parameter used for wind extrapolation from 10 m above the ground surface in the open, to 10 m above the canopy. (a) is for the open site simulation and (b) represents the open wind, the top-canopy extrapolated wind with $Z_{0f} = 4.5$ m and the open air temperature at 2 m (right y-axis). The ten half panels (c-l) show snowpack simulations for different Z_{0f} values and (l) is the value used for MEB/Crocus-new. Fluxes are stacked positively (surface gains energy) and negatively (surface losses energy) and the black line corresponds to the net final energy budget. All the years are available in https://zenodo.org/records/21264265 (Pauze et al., 2026a).

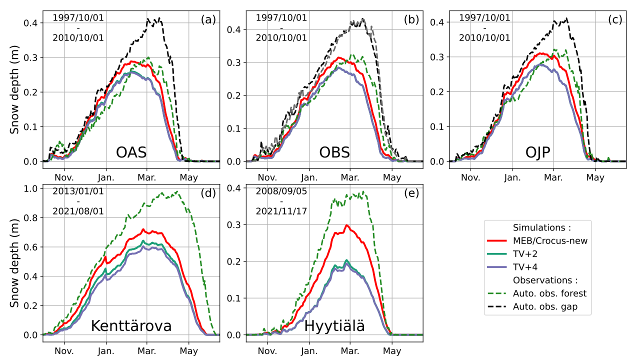

Figure C1. Average snow depth at the boreal sites. The simulations show the sensitivity of the model to an increase of the vegetation temperature threshold used to compute melt of intercepted snow. TV+2 is an increase by 2 °C and TV+4 is an increase by 4 °C. Year-by-year simulations are available in https://zenodo.org/records/21264265 (Pauze et al., 2026a).

Acknowledgements. The authors are grateful to Jean-Matthieu Monnet for help with the estimation of LAI from Lidar data, and for the LESSEM lab of INRAE for detailed characterization of the canopy at Col de Porte. They also thank Jean-Emmanuel Sicart, Benjamin Bouchard and Emmanuelle Barrette for the interesting discussion at EGU2026. Authors thank Léon Roussel for the help during the manual interception observations.

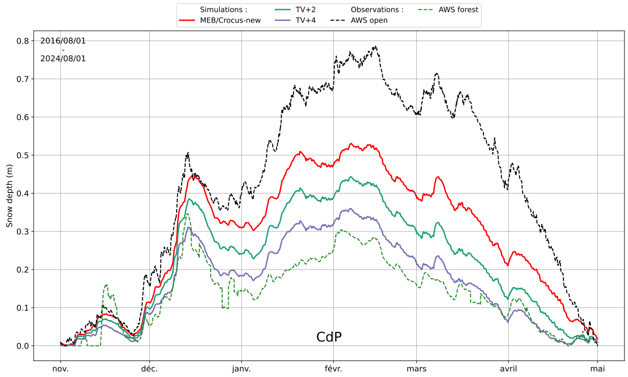

Figure C2. Average snow depth at Col de Porte over 2016 to 2024. The simulations show the sensitivity of the model to the increase of the vegetation temperature used to compute melt of intercepted snow. TV+2 is an increase by 2 °C and TV+4 is an increase by 4 °C. Year-by-year simulations are available in https://zenodo.org/records/21264265 (Pauze et al., 2026a).

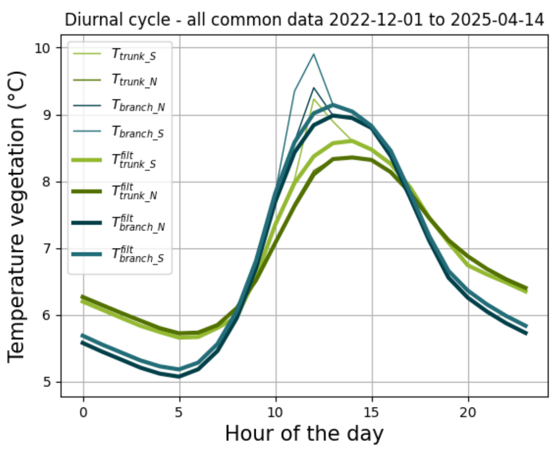

Figure D1. Diurnal cycle of vegetation temperatures measured at Col de Porte. Fine lines represent raw data while thick lines represent the filtered data where observations at 11am and 12am have been removed and replaced by a quadratic interpolation. The spike in raw data corresponds to direct sunlight reaching the sensors.

This research was supported by the French Meteorological Institute Meteo-France, Institut Polytechnique Paris, Agence de l'Eau Rhône Méditerranée Corse through the HydroChartreuse project and LabEx OSUG@2020 (ANR10 LABX56) under the SOURIRE project research grant.

The Col de Porte instrumented site is part of the OZCAR Research Infrastructure through the GLACIOCLIM Observatory and receives financial support from OSUG, LabEx OSUG@2020 (ANR10 LABX56) and Météo-France.

No AI tools have been used to code or generate text for this manuscript.

https://doi.org/10.5194/egusphere-2026-4137
Preprint. Discussion started: 1 September 2026

References

Abe, M., Takata, K., Kawamiya, M., and Watanabe, S.: Vegetation masking effect on future warming and snow albedo feedback in a boreal forest region of northern Eurasia according to MIROC-ESM, 122, 9245–9261, https://doi.org/10.1002/2017JD026957, 2017.

Andreadis, K. M., Storck, P., and Lettenmaier, D. P.: Modeling snow accumulation and ablation processes in forested environments, 45, https://doi.org/10.1029/2008WR007042, 2009.

Armstrong, R. L., Rittger, K., Brodzik, M. J., Racoviteanu, A., Barrett, A. P., Khalsa, S.-J. S., Raup, B., Hill, A. F., Khan, A. L., Wilson, A. M., Kayastha, R. B., Fetterer, F., and Armstrong, B.: Runoff from glacier ice and seasonal snow in High Asia: separating melt water sources in river flow, 19, 1249–1261, https://doi.org/10.1007/s10113-018-1429-0, 2019.

Barnett, T. P., Adam, J. C., and Lettenmaier, D. P.: Potential impacts of a warming climate on water availability in snow-dominated regions, 438, 303–309, https://doi.org/10.1038/nature04141, 2005.

Bartlett, P. A., MacKay, M. D., and Verseghy, D. L.: Modified snow algorithms in the Canadian land surface scheme: Model runs and sensitivity analysis at three boreal forest stands, https://doi.org/10.3137/ao.440301, 2006.

Boone, A. and Etchevers, P.: An Intercomparison of Three Snow Schemes of Varying Complexity Coupled to the Same Land Surface Model: Local-Scale Evaluation at an Alpine Site, 2, 374–394, https://doi.org/10.1175/1525-7541(2001)002<0374:AIOTSS>2.0.CO;2, 2001.

Boone, A., Samuelsson, P., Gollvik, S., Napoly, A., Jarlan, L., Brun, E., and Decharme, B.: The interactions between soil–biosphere–atmosphere land surface model with a multi-energy balance (ISBA-MEB) option in SURFEXv8 – Part 1: Model description, 10, 843–872, https://doi.org/10.5194/gmd-10-843-2017, 2017.

Bouchard, B., Nadeau, D. F., and Domine, F.: Comparison of snowpack structure in gaps and under the canopy in a humid boreal forest, 36, e14 681, https://doi.org/10.1002/hyp.14681, 2022.

Bouvier, M., Durrieu, S., Fournier, R. A., and Renaud, J.-P.: Generalizing predictive models of forest inventory attributes using an area-based approach with airborne LiDAR data, 156, 322–334, https://doi.org/10.1016/j.rse.2014.10.004, 2015.

Brun, E., Martin, , Simon, V., Gendre, C., and Coleou, C.: An Energy and Mass Model of Snow Cover Suitable for Operational Avalanche Forecasting, 35, 333–342, https://doi.org/10.3189/S0022143000009254, 1989.

Brun, E., David, P., Sudul, M., and Brunot, G.: A numerical model to simulate snow-cover stratigraphy for operational avalanche forecasting, 38, 13–22, https://doi.org/10.3189/S0022143000009552, 1992.

Bründl, M., Bartelt, P., Schneebeli, M., and Flühler, H.: Measuring branch deflection of spruce branches caused by intercepted snow load, 13, 2357–2369, https://doi.org/10.1002/(SICI)1099-1085(199910)13:14/15<2357::AID-HYP851>3.0.CO;2-O, 1999.

Cebulski, A. C. and Pomeroy, J. W.: Snow Interception Relationships With Meteorology and Canopy Density, 39, e70 135, https://doi.org/10.1002/hyp.70135, 2025.

Cebulski, A. C. and Pomeroy, J. W.: Processes Governing the Ablation of Intercepted Snow, 62, e2025WR042 009, https://doi.org/10.1029/2025WR042009, 2026.

Clark, M. P., Nijssen, B., Lundquist, J. D., Kavetski, D., Rupp, D. E., Woods, R. A., Freer, J. E., Gutmann, E. D., Wood, A. W., Gochis, D. J., Rasmussen, R. M., Tarboton, D. G., Mahat, V., Flerchinger, G. N., and Marks, D. G.: A unified approach for process-based hydrologic modeling: 2. Model implementation and case studies, 51, 2515–2542, https://doi.org/10.1002/2015WR017200, 2015.

Decharme, B., Brun, E., Boone, A., Delire, C., Le Moigne, P., and Morin, S.: Impacts of snow and organic soils parameterization on northern Eurasian soil temperature profiles simulated by the ISBA land surface model, 10, 853–877, https://doi.org/10.5194/tc-10-853-2016, 2016.

https://doi.org/10.5194/egusphere-2026-4137
Preprint. Discussion started: 1 September 2026

Deschamps-Berger, C., López-Moreno, J. I., Gascoin, S., Mazzotti, G., and Boone, A.: Where Snow and Forest Meet: A Global Atlas, 52, e2024GL113 684, https://doi.org/10.1029/2024GL113684, 2025.

Dick, O., Viallon-Galinier, L., Tuzet, F., Hagenmuller, P., Fructus, M., Reuter, B., Lafaysse, M., and Dumont, M.: Can Saharan dust deposition impact snowpack stability in the French Alps?, 17, 1755–1773, https://doi.org/10.5194/tc-17-1755-2023, 2023.

Essery, R.: A factorial snowpack model (FSM 1.0), 8, 3867–3876, https://doi.org/10.5194/gmd-8-3867-2015, 2015.

Essery, R., Rutter, N., Pomeroy, J., Baxter, R., Stähli, M., Gustafsson, D., Barr, A., Bartlett, P., and Elder, K.: SNOWMIP2: An Evaluation of Forest Snow Process Simulations, 90, 1120–1136, https://doi.org/10.1175/2009BAMS2629.1, 2009.

Etchevers, P., Martin, E., Brown, R., Fierz, C., Lejeune, Y., Bazile, E., Boone, A., Dai, Y.-J., Essery, R., Fernandez, A., Gusev, Y., Jordan, R., Koren, V., Kowalczyk, E., Nasonova, N. O., Pyles, R. D., Schlosser, A., Shmakin, A. B., Smirnova, T. G., Strasser, U., Verseghy, D., Yamazaki, T., and Yang, Z.-L.: Validation of the energy budget of an alpine snowpack simulated by several snow models (Snow MIP project), 38, 150–158, https://doi.org/10.3189/172756404781814825, 2004.

Flanner, M. G., Shell, K. M., Barlage, M., Perovich, D. K., and Tschudi, M. A.: Radiative forcing and albedo feedback from the Northern Hemisphere cryosphere between 1979 and 2008, 4, 151–155, https://doi.org/10.1038/ngeo1062, 2011.

Forland, E., Allerup, P., Dahlström, B., Elomaa, E., Jonsson, J., Madsen, H., Perälä, J., Rissanan, P., Vedin, H., and Vejen, F.: Manual for operational correction of Nordic precipitation data, 1996.

Gouttevin, I., Lehning, M., Jonas, T., Gustafsson, D., and Mölder, M.: A two-layer canopy model with thermal inertia for an improved snowpack energy balance below needleleaf forest (model SNOWPACK, version 3.2.1, revision 741), 8, 2379–2398, https://doi.org/10.5194/gmd-8-2379-2015, 2015.

Gouttevin, I., Vionnet, V., Seity, Y., Boone, A., Lafaysse, M., Deliot, Y., and Merzisen, H.: To the Origin of a Wintertime Screen-Level Temperature Bias at High Altitude in a Kilometric NWP Model, 24, 53–71, https://doi.org/10.1175/JHM-D-21-0200.1, 2023.

Hedstrom, N. R. and Pomeroy, J. W.: Measurements and modelling of snow interception in the boreal forest, 12, 1611–1625, https://doi.org/10.1002/(SICI)1099-1085(199808/09)12:10/11<1611::AID-HYP684>3.0.CO;2-4, 1998.

Helbig, N., Moeser, D., Teich, M., Vincent, L., Lejeune, Y., Sicart, J.-E., and Monnet, J.-M.: Snow processes in mountain forests: interception modeling for coarse-scale applications, 24, 2545–2560, https://doi.org/10.5194/hess-24-2545-2020, 2020.

Kamoske, A. G., Dahlin, K. M., Stark, S. C., and Serbin, S. P.: Leaf area density from airborne LiDAR: Comparing sensors and resolutions in a temperate broadleaf forest ecosystem, 433, 364–375, https://doi.org/10.1016/j.foreco.2018.11.017, 2019.

Kittredge, J.: Influences of forests on snow in the ponderosa-sugar pine-fir zone of the central Sierra Nevada, https://ageconsearch.umn.edu/record/381670, 1953.

Kobayashi, D.: Snow accumulation on a narrow board, 13, 239–245, https://doi.org/10.1016/0165-232X(87)90005-X, 1987.

Krinner, G., Derksen, C., Essery, R., Flanner, M., Hagemann, S., Clark, M., Hall, A., Rott, H., Brutel-Vuilmet, C., Kim, H., Ménard, C. B., Mudryk, L., Thackeray, C., Wang, L., Arduini, G., Balsamo, G., Bartlett, P., Boike, J., Boone, A., Chéruy, F., Colin, J., Cuntz, M., Dai, Y., Decharme, B., Derry, J., Ducharne, A., Dutra, E., Fang, X., Fierz, C., Ghattas, J., Gusev, Y., Haverd, V., Kontu, A., Lafaysse, M., Law, R., Lawrence, D., Li, W., Marke, T., Marks, D., Ménégoz, M., Nasonova, O., Nitta, T., Niwano, M., Pomeroy, J., Raleigh, M. S., Schaedler, G., Semenov, V., Smirnova, T. G., Stacke, T., Strasser, U., Svenson, S., Turkov, D., Wang, T., Wever, N., Yuan, H., Zhou, W., and Zhu, D.: ESM-SnowMIP: assessing snow models and quantifying snow-related climate feedbacks, 11, 5027–5049, https://doi.org/10.5194/gmd-11-5027-2018, 2018.

Lafaysse, M., Cluzet, B., Dumont, M., Lejeune, Y., Vionnet, V., and Morin, S.: A multiphysical ensemble system of numerical snow modelling, 11, 1173–1198, https://doi.org/10.5194/tc-11-1173-2017, 2017.

https://doi.org/10.5194/egusphere-2026-4137
Preprint. Discussion started: 1 September 2026

Lafaysse, M., Dumont, M., De Fleurian, B., Fructus, M., Nheili, R., Viallon-Galinier, L., Baron, M., Boone, A., Bouchet, A., Brondex, J., Carmagnola, C., Cluzet, B., Fourteau, K., Haddjeri, A., Hagenmuller, P., Mazzotti, G., Minvielle, M., Morin, S., Quéno, L., Roussel, L., Spandre, P., Tuzet, F., and Vionnet, V.: Version 3.0 of the Crocus snowpack model, pp. 1–75, https://doi.org/10.5194/egusphere-2025-4540, 2025.

Lawrence, D. M., Fisher, R. A., Koven, C. D., Oleson, K. W., Swenson, S. C., Bonan, G., Collier, N., Ghimire, B., van Kampenhout, L., Kennedy, D., Kluzek, E., Lawrence, P. J., Li, F., Li, H., Lombardozzi, D., Riley, W. J., Sacks, W. J., Shi, M., Vertenstein, M., Wieder, W. R., Xu, C., Ali, A. A., Badger, A. M., Bisht, G., van den Broeke, M., Brunke, M. A., Burns, S. P., Buzan, J., Clark, M., Craig, A., Dahlin, K., Drewniak, B., Fisher, J. B., Flanner, M., Fox, A. M., Gentine, P., Hoffman, F., Keppel-Aleks, G., Knox, R., Kumar, S., Lenaerts, J., Leung, L. R., Lipscomb, W. H., Lu, Y., Pandey, A., Pelletier, J. D., Perket, J., Randerson, J. T., Ricciuto, D. M., Sanderson, B. M., Slater, A., Subin, Z. M., Tang, J., Thomas, R. Q., Val Martin, M., and Zeng, X.: The Community Land Model Version 5: Description of New Features, Benchmarking, and Impact of Forcing Uncertainty, 11, 4245–4287, https://doi.org/10.1029/2018MS001583, 2019.

Lejeune, Y., Dumont, M., Panel, J.-M., Lafaysse, M., Lapalus, P., Le Gac, E., Lesaffre, B., and Morin, S.: 57 years (1960–2017) of snow and meteorological observations from a mid-altitude mountain site (Col de Porte, France, 1325\,m of altitude), 11, 71–88, https://doi.org/10.5194/essd-11-71-2019, 2019.

Li, D., Wrzesien, M. L., Durand, M., Adam, J., and Lettenmaier, D. P.: How much runoff originates as snow in the western United States, and how will that change in the future?, 44, 6163–6172, https://doi.org/10.1002/2017GL073551, 2017.

Lundquist, J. D., Dickerson-Lange, S., Gutmann, E., Jonas, T., Lumbrazo, C., and Reynolds, D.: Snow interception modelling: Isolated observations have led to many land surface models lacking appropriate temperature sensitivities, 35, e14 274, https://doi.org/10.1002/hyp.14274, 2021.

Mahat, V. and Tarboton, D. G.: Representation of canopy snow interception, unloading and melt in a parsimonious snowmelt model, 28, 6320–6336, https://doi.org/10.1002/hyp.10116, 2014.

Masson, V., Le Moigne, P., Martin, E., Faroux, S., Alias, A., Alkama, R., Belamari, S., Barbu, A., Boone, A., Bouyssel, F., Brousseau, P., Brun, E., Calvet, J.-C., Carrer, D., Decharme, B., Delire, C., Donier, S., Essaouini, K., Gibelin, A.-L., Giordani, H., Habets, F., Jidane, M., Kerdraon, G., Kourzeneva, E., Lafaysse, M., Lafont, S., Lebeaupin Brossier, C., Lemonsu, A., Mahfouf, J.-F., Marguinaud, P., Mokhtari, M., Morin, S., Pigeon, G., Salgado, R., Seity, Y., Taillefer, F., Tanguy, G., Tulet, P., Vincendon, B., Vionnet, V., and Voldoire, A.: The SURFEXv7.2 land and ocean surface platform for coupled or offline simulation of earth surface variables and fluxes, 6, 929–960, https://doi.org/10.5194/gmd-6-929-2013, 2013.

Mazzotti, G., Currier, W. R., Deems, J. S., Pflug, J. M., Lundquist, J. D., and Jonas, T.: Revisiting Snow Cover Variability and Canopy Structure Within Forest Stands: Insights From Airborne Lidar Data, 55, 6198–6216, https://doi.org/10.1029/2019WR024898, 2019.

Mazzotti, G., Essery, R., Moeser, C. D., and Jonas, T.: Resolving Small-Scale Forest Snow Patterns Using an Energy Balance Snow Model With a One-Layer Canopy, 56, e2019WR026 129, https://doi.org/10.1029/2019WR026129, 2020a.

Mazzotti, G., Essery, R., Webster, C., Malle, J., and Jonas, T.: Process-Level Evaluation of a Hyper-Resolution Forest Snow Model Using Distributed Multisensor Observations, 56, e2020WR027 572, https://doi.org/10.1029/2020WR027572, 2020b.

Mazzotti, G., Vaccaro, F., Courteaud, A., Fructus, M., Magnusson, J., Gouttevin, I., Nousu, J.-P., and Lafaysse, M.: Assessing spatially distributed snow simulations with MEB-Crocus in subalpine forests through modelling experiments, pp. 1–33, https://doi.org/10.5194/egusphere-2026-1464, 2026.

Molotch, N. P., Brooks, P. D., Burns, S. P., Litvak, M., Monson, R. K., McConnell, J. R., and Musselman, K.: Ecohydrological controls on snowmelt partitioning in mixed-conifer sub-alpine forests, 2, 129–142, https://doi.org/10.1002/eco.48, 2009.

https://doi.org/10.5194/egusphere-2026-4137
Preprint. Discussion started: 1 September 2026

Molotch, N. P., Barnard, D. M., Burns, S. P., and Painter, T. H.: Measuring spatiotemporal variation in snow optical grain size under a subalpine forest canopy using contact spectroscopy, 52, 7513–7522, https://doi.org/10.1002/2016WR018954, 2016.

Morin, S., Samacoïts, R., François, H., Carmagnola, C. M., Abegg, B., Demiroglu, O. C., Pons, M., Soubeyroux, J.-M., Lafaysse, M., Franklin, S., Griffiths, G., Kite, D., Hoppler, A. A., George, E., Buontempo, C., Almond, S., Dubois, G., and Cauchy, A.: Pan-European meteorological and snow indicators of climate change impact on ski tourism, 22, 100 215, https://doi.org/10.1016/j.cliser.2021.100215, 2021.

Ménard, C. B., Essery, R., Barr, A., Bartlett, P., Derry, J., Dumont, M., Fierz, C., Kim, H., Kontu, A., Lejeune, Y., Marks, D., Niwano, M., Raleigh, M., Wang, L., and Wever, N.: Meteorological and evaluation datasets for snow modelling at 10 reference sites: description of in situ and bias-corrected reanalysis data, 11, 865–880, https://doi.org/10.5194/essd-11-865-2019, 2019.

Napoly, A., Boone, A., and Welfringer, T.: ISBA-MEB (SURFEX v8.1): model snow evaluation for local-scale forest sites, 13, 6523–6545, https://doi.org/10.5194/gmd-13-6523-2020, 2020.

Nitu, R., Roulet, Y.-A., Wolff, M., Earle, M. E., Reverdin, A., Smith, C. D., Kochendorfer, J., Morin, S., Rasmussen, R., Wong, K., Alastrué Tierra, J. J., Arnold, L., Baker, B., Buisán Sanz, S. T., Collado Aceituno, J. L., Colli, M., Collins, B., Gaydos, A., Hannula, H.-R., Hoover, J., Joe, P., Kontu, A., Laine, T., Lanza, L., Lanzinger, E., Lee, G., Lejeune, Y., Leppänen, L., Mekis, E., Panel, J.-M., Poikonen, A., Ryu, S., Sabatini, F., Thériault, J. M., Yang, D., Genthon, C., Heuvel, F. v. d., Hirasawa, N., Konishi, H., Motoyoshi, H., Nakai, S., Nishimura, K., Senese, A., and Yamashita, K.: WMO Solid Precipitation Intercomparison Experiment (SPICE) (2012 - 2015), https://repositorio.aemet.es/handle/20.500.11765/10839, 2019.

Niu, G.-Y. and Yang, Z.-L.: Effects of vegetation canopy processes on snow surface energy and mass balances, 109, https://doi.org/10.1029/2004JD004884, 2004.

Nousu, J.-P., Lafaysse, M., Mazzotti, G., Ala-aho, P., Marttila, H., Cluzet, B., Aurela, M., Lohila, A., Kolari, P., Boone, A., Fructus, M., and Launiainen, S.: Modeling snowpack dynamics and surface energy budget in boreal and subarctic peatlands and forests, 18, 231–263, https://doi.org/10.5194/tc-18-231-2024, 2024.

Pauze, T., Bouchet, A., Gouttevin, I., Boone, A., Fructus, M., Lafaysse, M., Le Gac, E., Rivière, A., and Lejeune, Y.: Supplement to : Improvements of a subcanopy snow model and its interception conveyed by observations from a mid-altitude alpine site, https://doi.org/10.5281/zenodo.21264265, 2026a.

Pauze, T., Bouchet, A., Gouttevin, I., Boone, A., Fructus, M., Lafaysse, M., Le Gac, E., Rivière, A., and Lejeune, Y.: SURFEX software supplement for "Improvements of a subcanopy snow model and its interception conveyed by observations from a mid-altitude alpine site", https://doi.org/10.5281/zenodo.21263777, 2026b.

Pomeroy, J. W., Parviainen, J., Hedstrom, N., and Gray, D. M.: Coupled modelling of forest snow interception and sublimation, 12, 2317–2337, https://doi.org/10.1002/(SICI)1099-1085(199812)12:15<2317::AID-HYP799>3.0.CO;2-X, 1998.

Roesch, A., Wild, M., Gilgen, H., and Ohmura, A.: A new snow cover fraction parametrization for the ECHAM4 GCM, 17, 933–946, https://doi.org/10.1007/s003820100153, 2001.

Roth, T. R. and Nolin, A. W.: Characterizing Maritime Snow Canopy Interception in Forested Mountains, 55, 4564–4581, https://doi.org/10.1029/2018WR024089, 2019.

Roussel, J.-R., Auty, D., Coops, N. C., Tompalski, P., Goodbody, T. R. H., Meador, A. S., Bourdon, J.-F., de Boissieu, F., and Achim, A.: lidR: An R package for analysis of Airborne Laser Scanning (ALS) data, 251, 112 061, https://doi.org/10.1016/j.rse.2020.112061, 2020.

Roussel, L., Dumont, M., Gascoin, S., Monteiro, D., Bavay, M., Nabat, P., Ezzedine, J. A., Fructus, M., Lafaysse, M., Morin, S., and Maréchal, E.: Snowmelt duration controls red algal blooms in the snow of the European Alps, 121, e2400362 121, https://doi.org/10.1073/pnas.2400362121, 2024.

Rutter, N., Essery, R., Pomeroy, J., Altimir, N., Andreadis, K., Baker, I., Barr, A., Bartlett, P., Boone, A., Deng, H., Douville, H., Dutra, E., Elder, K., Ellis, C., Feng, X., Gelfan, A., Goodbody, A., Gusev, Y., Gustafsson, D., Hellström, R., Hirabayashi, Y., Hirota, T., Jonas, T., Koren, V., Kuragina, A., Lettenmaier, D., Li, W.-P., Luce, C., Martin, E., Nasonova, O., Pumpanen, J., Pyles, R. D., Samuelsson, P., Sandells, M., Schädler, G., Shmakin, A., Smirnova, T. G., Stähli, M., Stöckli, R., Strasser, U., Su, H., Suzuki, K., Takata, K., Tanaka, K., Thompson, E., Vesala, T., Viterbo, P., Wiltshire, A., Xia, K., Xue, Y., and Yamazaki, T.: Evaluation of forest snow processes models (SnowMIP2), 114, https://doi.org/10.1029/2008JD011063, 2009.

Réveillet, M., Dumont, M., Gascoin, S., Lafaysse, M., Nabat, P., Ribes, A., Nheili, R., Tuzet, F., Ménégoz, M., Morin, S., Picard, G., and Ginoux, P.: Black carbon and dust alter the response of mountain snow cover under climate change, 13, 5279, https://doi.org/10.1038/s41467-022-32501-y, 2022.

Satterlund, D. R. and Haupt, H. F.: Snow catch by Contier Crowns, 3, 1035–1039, https://doi.org/10.1029/WR003i004p01035, 1967.

Schmidt, R. A. and Gluns, D. R.: Snowfall interception on branches of three conifer species, 21, 1262–1269, https://doi.org/10.1139/x91-176, 1991.

Schmidt, R. A. and Pomeroy, J. W.: Bending of a conifer branch at subfreezing temperatures: implications for snow interception, 20, 1251–1253, https://doi.org/10.1139/x90-165, 1990.

Seity, Y., Brousseau, P., Malardel, S., Hello, G., Bénard, P., Bouttier, F., Lac, C., and Masson, V.: The AROME-France Convective-Scale Operational Model, 139, 976–991, https://doi.org/10.1175/2010MWR3425.1, 2011.

Sicart, J., Ramseyer, V., Picard, G., Arnaud, L., Coulaud, C., Freche, G., Soubeyrand, D., Lejeune, Y., Dumont, M., Gouttevin, I., Gac, E., Berger, F., Monnet, J.-M., Borgniet, L., Mermin, , Rutter, N., Webster, C., and Essery, R.: Snow accumulation and ablation measurements in a midlatitude mountain coniferous forest (Col de Porte, France, 1325 m altitude): the Snow Under Forest (SnoUF) field campaign data set, 15, 5121–5133, https://doi.org/10.5194/essd-15-5121-2023, 2023.

Stewart, I. T.: Changes in snowpack and snowmelt runoff for key mountain regions, 23, 78–94, https://doi.org/10.1002/hyp.7128, 2009.

Stewart, I. T., Cayan, D. R., and Dettinger, M. D.: Changes in Snowmelt Runoff Timing in Western North America under a 'Business as Usual' Climate Change Scenario, 62, 217–232, https://doi.org/10.1023/B:CLIM.0000013702.22656.e8, 2004.

Storck, P.: Trees, snow and flooding: an investigation of forest canopy effects on snow accumulation and melt at the plot and watershed scales in the Pacific Northwest, publisher: Washington State University Department of Civil and Environmental Engineering, 2000.

Storck, P., Lettenmaier, D. P., and Bolton, S. M.: Measurement of snow interception and canopy effects on snow accumulation and melt in a mountainous maritime climate, Oregon, United States, 38, 5–1–5–16, https://doi.org/10.1029/2002WR001281, 2002.

Tanner, C. B. and Pelton, W. L.: Potential evapotranspiration estimates by the approximate energy balance method of Penman, 65, 3391–3413, https://doi.org/10.1029/JZ065i010p03391, 1960.

Thackeray, C. W., Fletcher, C. G., and Derksen, C.: The influence of canopy snow parameterizations on snow albedo feedback in boreal forest regions, 119, 9810–9821, https://doi.org/10.1002/2014JD021858, 2014.

Thom, A. S.: Momentum absorption by vegetation, 97, 414–428, https://doi.org/10.1002/qj.49709741404, 1971.

Vernay, M., Lafaysse, M., Monteiro, D., Hagenmuller, P., Nheili, R., Samacoïts, R., Verfaillie, D., and Morin, S.: The S2M meteorological and snow cover reanalysis over the French mountainous areas: description and evaluation (1958–2021), 14, 1707–1733, https://doi.org/10.5194/essd-14-1707-2022, 2022.

Vincent, L., Lejeune, Y., Boone, A., Gac, E. L., Coulaud, C., Freche, G., and Sicart, J.-E.: Interception of snowfall by the trees is the main challenge for snowpack simulations under forests, 2018.

Webster, C., Rutter, N., Zahner, F., and Jonas, T.: Measurement of Incoming Radiation below Forest Canopies: A Comparison of Different Radiometer Configurations, 17, 853–864, https://doi.org/10.1175/JHM-D-15-0125.1, 2016a.

Webster, C., Rutter, N., Zahner, F., and Jonas, T.: Modeling subcanopy incoming longwave radiation to seasonal snow using air and tree trunk temperatures, 121, 1220–1235, https://doi.org/10.1002/2015JD024099, 2016b.

Webster, C., Rutter, N., and Jonas, T.: Improving representation of canopy temperatures for modeling subcanopy incoming longwave radiation to the snow surface, 122, 9154–9172, https://doi.org/10.1002/2017JD026581, 2017.